

GRP78 and Integrins Play Different Roles in Host Cell Invasion During Mucormycosis

Abdullah Alqarihi,^a Teclegiorgis Gebremariam,^a Yiyu Gu,^a Marc Swidergall,^{a,b} Sondus Alkhazraji,^a
Sameh S.M. Soliman,^c Vincent M. Bruno,^d John E. Edwards, Jr.,^{a,b} Scott G. Filler,^{a,b} Priya Uppuluri,^{a,b}
Ashraf S. Ibrahim^{a,b,#}

Division of Infectious Diseases, The Lundquist Institute for Biomedical Innovation at Harbor-University of California Los Angeles (UCLA) Medical Center, Torrance, California, USA^a; David Geffen School of Medicine at UCLA, Los Angeles, California, USA^b; Research Institute For Medical and Health Sciences, and College of Pharmacy, University of Sharjah, Sharjah, P.O. Box 27272, United Arab Emirates^c; Institute for Genome Sciences, University of Maryland School of Medicine, Baltimore, Maryland, USA^d.

Running Title: GRP78 and Integrin host receptors during mucormycosis

Keywords: GRP78, integrin β 1, *Rhizopus*, mucormycosis, cell invasion, epithelial cells

[#]Address correspondence to Ashraf S. Ibrahim, ibrahim@lundquist.org.

21 **Abstract**

22 Mucormycosis, caused by *Rhizopus* species, is a life-threatening fungal infection that occurs in patients
23 immunocompromised by diabetic ketoacidosis (DKA), cytotoxic chemotherapy, immunosuppressive therapy,
24 hematologic malignancies or severe trauma. Inhaled *Rhizopus* spores cause pulmonary infections in patients
25 with hematologic malignancies, while patients with DKA are much more prone to rhinoorbital/cerebral
26 mucormycosis. Here we show that *R. delemar* interacts with glucose-regulated protein 78 (GRP78) on nasal
27 epithelial cells via its spore coat protein CotH3 to invade and damage the nasal epithelial cell. Expression of the
28 two proteins is significantly enhanced by high glucose, iron and ketone body levels (hallmark features of DKA),
29 potentially leading to frequently lethal rhinoorbital/cerebral mucormycosis. In contrast, *R. delemar* CotH7
30 recognizes integrin $\beta 1$ as a receptor on alveolar epithelial cells causing the activation of epidermal growth factor
31 receptor (EGFR) leading to host cell invasion. Anti-integrin $\beta 1$ antibodies inhibit *R. delemar* invasion of
32 alveolar epithelial cells and protect mice from pulmonary mucormycosis. Our results show that *R. delemar*
33 interacts with different mammalian receptors depending on the host cell type. Susceptibility of patients with
34 DKA primarily to rhinoorbital/cerebral disease can be explained by host factors typically present in DKA and
35 known to upregulate CotH3 and nasal GRP78 thereby trapping the fungal cells within the rhino-orbital milieu,
36 leading to subsequent invasion and damage. Our studies highlight that mucormycosis pathogenesis can
37 potentially be overcome by the development of novel customized therapies targeting niche-specific host
38 receptors or their respective fungal ligands.

39

40 Word count: 238

41

42

43

44

45

46 **Importance**

47

48 Mucormycosis caused by *Rhizopus* species is a fungal infection with often fatal prognosis. Inhalation of

49 spores is the major route of entry, with nasal and alveolar epithelial cells among the first cells that encounter the

50 fungi. In patients with hematologic malignancies or those undergoing cytotoxic chemotherapy, *Rhizopus* causes

51 pulmonary infections. On the other hand, DKA patients predominantly suffer from rhinoorbital/cerebral

52 mucormycosis. The reason for such disparity in disease types by the same fungus is not known. Here we show

53 that, the unique susceptibility of DKA subjects to rhinoorbital/cerebral mucormycosis is likely due to specific

54 interaction between nasal epithelial cell GRP78 and fungal CotH3, the expression of which increase in the

55 presence of host factors present in DKA. In contrast, pulmonary mucormycosis is initiated via interaction of

56 inhaled spores expressing CotH7 with integrin β 1 receptor which activates EGFR to induce fungal invasion of

57 host cells. These results introduce plausible explanation to disparate disease manifestations in DKA versus

58 hematologic malignancy patients and provide a foundation for development of therapeutic interventions against

59 these lethal forms of mucormycosis.

60

61

62 **Introduction**

63 Mucormycosis is a lethal infection caused by mold belonging to the order Mucorales (1, 2). The infection is
64 characterized by high degree of angioinvasion which results in substantial tissue necrosis, frequently mandating
65 surgical debridement of infected tissues (3, 4). Despite aggressive treatment with surgical removal of infected
66 foci and use of the limited options of antifungal agents, mucormycosis is associated with dismal mortality rates
67 of 50-100% (5, 6). Also, surviving patients often require major reconstructive surgeries to manage the ensuing
68 highly disfiguring defects (2, 7).

69 *Rhizopus* spp. are the most common etiologic agents of mucormycosis, responsible for approximately
70 70% of all cases (1, 2, 6). Other isolated organisms belong to the genera *Mucor*, and *Rhizomucor*; while fungi
71 such as *Cunninghamella*, *Lichthemia*, and *Apophysomyces* less commonly cause infection (6). These organisms
72 are ubiquitous in nature, found on decomposing vegetation and soil, where they grow rapidly and release large
73 numbers of spores that can become airborne. While spores are generally harmless to immunocompetent people,
74 almost all human infections occur in the presence of some underlying immunocompromising condition. These
75 include hematological malignancies, organ or bone marrow transplant, corticosteroids use, hyperglycemia,
76 diabetic ketoacidosis (DKA), and other forms of acidosis (2, 4, 8). Immunocompetent individuals suffering
77 from burn wounds or severe trauma (e.g. soldiers in combat operations and motorcycle accident victims), or
78 those injured in the aftermath of natural disasters (e.g., the Southeast Asian tsunami in 2004, or the tornadoes in
79 Joplin, Missouri, in June 2011), are also uniquely susceptible to life-threatening Mucorales infections (9-11).

80 Devastating rhinoorbital/cerebral and pulmonary mucormycosis are the most common manifestations of
81 the infection caused by inhalation of spores (8, 12). In healthy individuals, cilia carry spores to the pharynx,
82 which are later cleared through the gastrointestinal tract (13). Diabetes is a risk factor that predominantly
83 predisposes individuals to rhinoorbital/cerebral mucormycosis (RCM) (6, 8). In susceptible individuals, RCM
84 usually begins in the paranasal sinuses, where the organisms adhere to and proliferate in the nasal epithelial
85 cells. Eventually, adhered Mucorales invade adjoining areas such as the palate, the orbit, and the brain, causing
86 extensive necrosis, destruction of nasal turbinates', cranial nerve palsies and facial disfigurement, all in a short

87 span of days to weeks. Due to the angioinvasive nature of the disease, the infection often hematogenously
88 disseminates to infect distant organs. We have shown that *Rhizopus* thrives in high glucose, and acidic
89 conditions and can invade human umbilical vein endothelial cells via interaction of the fungal ligand, spore-coat
90 protein (CotH), with the host cell receptor glucose regulated protein 78 kDa protein (GRP78) (14, 15). In
91 contrast, in neutropenic patients inhaled spores can directly progress into the bronchioles and alveoli causing
92 pneumonia and rarely cause RCM (16-18). The reasons why patients with DKA are mainly infected with RCM,
93 whereas neutropenic patients commonly suffer from pulmonary infections (8, 19) are not understood. We
94 postulate that Mucorales ligands recognize host receptors unique to individual cell types (i.e. alveolar, nasal,
95 endothelial cells), and that this fungal ligand-host receptor interaction is enhanced by host factors, eventually
96 leading to infections in the respective host niches.

97 To investigate this hypothesis, we identified the nasal and alveolar epithelial cell receptors to Mucorales
98 ligands and studied the effect of host factors commonly present in DKA patients on the expression and
99 interaction of these receptors/ligands. Here we show that, similar to endothelial cells, the fungal CotH3 protein
100 physically interacts with GRP78 on nasal epithelial cells. Elevated concentrations of glucose, iron and ketone
101 bodies present during DKA significantly induce the expression of GRP78 and CotH3, leading to enhanced
102 invasion and damage of nasal epithelial cells. Antibodies against either CotH3 or GRP78 abrogate *R. delemar*
103 invasion and damage of nasal epithelial cells. In contrast, *Rhizopus* binds to integrin $\beta 1$ during invasion of
104 alveolar epithelial cells. Binding to integrin $\beta 1$ triggers the activation of epidermal growth factor receptor
105 (EGFR) signaling (20). Anti-integrin $\beta 1$ antibodies significantly reduce EGFR activation, blocks alveolar
106 epithelial cell invasion and protect neutropenic mice from pulmonary mucormycosis. These results introduce
107 plausible explanation for the unique susceptibility of DKA patients to RCM in which inhaled Mucorales spores
108 are trapped in the sinuses via GRP78/CotH3 overexpression. We also posit that receptors identified in this study
109 are potential novel targets for development of pharmacologic or immunotherapeutic approaches against a
110 variety of extremely lethal mucormycosis infections.

112 Results

113 **Distinct host receptors are used by *R. delemar* to invade and damage nasal or alveolar epithelial cells.** We
114 compared the ability of *R. delemar* to invade and damage either nasal or alveolar A549 epithelial cells *in vitro*.
115 Incubation of *R. delemar* germlings with either of the two cell lines, resulted in ~40% invasion of host cells
116 within the first 3 h of interaction, and by 6 h, almost all germlings had invaded the nasal and alveolar epithelial
117 cells (**Fig. 1**). Interestingly, *R. delemar*-mediated damage of nasal epithelial cells occurred significantly earlier
118 than damage of alveolar epithelial cells. Specifically, fungal germlings damaged 40% and 80% of the nasal
119 epithelial cells within 30 h and 48 h, respectively (**Fig. 1A**). In contrast, no detectable damage and only 50% of
120 the alveolar epithelial cells were injured after similar periods of incubation with *R. delemar* (**Fig. 1B**). These
121 results also show that fungal invasion precedes damage of both types of epithelial cells. Importantly, *R.*
122 *delemar*-mediated damage of primary human alveolar epithelial cells was similar to damage caused to A549
123 cells (**Fig. S1**). Therefore, the invasion and damage of the alveolar epithelial cell line is reflective of *R. delemar*
124 interactions with primary alveolar epithelial cells.

125 We questioned if the disparity in damage to the two different epithelial cells was due to *R. delemar*'s
126 ability to recognize different host receptors on the nasal and alveolar epithelial cells. We used an affinity
127 purification process developed by Isberg and Leong (21), where *R. delemar* germlings were incubated
128 separately with extracts of biotin-labeled total proteins of the nasal or alveolar epithelial cells. *R. delemar*
129 specifically bound to a single nasal epithelial cell protein band that was isolated on an SDS-PAGE gel, and
130 observed as a 78 kDa band post immunoblotting with anti-biotin antibodies (**Fig. 2A**). This protein band was
131 identified by liquid chromatography–mass spectrometry (LC-MS) as the human GRP78, which we previously
132 reported to be a receptor to invading Mucorales on human umbilical vein endothelial cells (14). To confirm the
133 identity of the band, we stripped and probed the same immunoblot containing the nasal epithelial cell membrane
134 proteins with an anti-GRP78 polyclonal antibodies. The polyclonal antibodies recognized the 78-kDa band that
135 had bound to *R. delemar* germlings (**Fig. 2A**).

136 Similarly, only a single 130 kDa protein band from the alveolar epithelial cell extracts was bound to *R. delemar*
137 germlings (**Fig. 2B**). This protein was identified as integrin $\beta 1$ by LC-MS, and subsequently confirmed by
138 probing with an anti-integrin $\beta 1$ antibody on Western blotting (**Fig. 2B**). Integrins are known to be highly
139 expressed in human lung tissues (<https://www.ncbi.nlm.nih.gov/gene/3675>), and we found that gene expression
140 of integrin $\beta 1$, but not GRP78, was upregulated in alveolar epithelial cells during infection with *R. delemar*
141 (**Fig. S2**). Furthermore, transcriptomic analysis of mouse lung tissues in early stages of pulmonary
142 mucormycosis identified an upregulation of a gene encoding for integrin $\alpha 3$ (22). Since integrins function as
143 heterodimers (23), we sought to verify if integrin $\alpha 3$ subunit combines with integrin $\beta 1$ in acting as a putative
144 receptor to *R. delemar* by alveolar epithelial cells. An integrin $\alpha 3\beta 1$ polyclonal antibody recognized the 130
145 kDa band from A549 alveolar epithelial cells (**Fig. 2B**). Therefore, it is possible that $\alpha 3$ subunit functions as a
146 heterodimer with $\beta 1$ to serve as a receptor during Mucorales invasion of alveolar epithelial cells.

147 To investigate if nasal GRP78 and alveolar integrin $\alpha 3\beta 1$ are putative universal receptors to other
148 Mucorales, we performed the affinity purification experiment using germlings of other Mucorales clinical
149 isolates. Indeed, all tested Mucorales including *R. oryzae* 99-892, *M. circinelloides* 131, *Rhizomucor*, *C.*
150 *bertholletiae* 182 and *L. corymbifera* 008-0490 bound GRP78 and integrin $\alpha 3\beta 1$ from nasal (**Fig. 2C**) and
151 alveolar (**Fig. 2D**) epithelial cells, respectively. Collectively, these data suggest that Mucorales interacts with
152 nasal and alveolar epithelial cells by using different host receptors.

153

154 **GRP78 and integrin $\beta 1$ are receptors on nasal and alveolar epithelial cells, respectively.** To confirm the
155 function of GRP78 and integrin $\beta 1$ on nasal and alveolar epithelial cells as receptors to *R. delemar*, we
156 examined the effect of anti-GRP78 and anti-integrin $\beta 1$ antibodies on *R. delemar*-mediated host cell adhesion,
157 invasion and subsequent damage. While incubating nasal epithelial cells with anti-GRP78 polyclonal antibodies
158 resulted in ~50% inhibition of *R. delemar*-mediated host cell invasion, the antibodies had no effect on adhesion
159 when compared to isotype-matched control antibodies (**Fig. 2E**). The anti-GRP78 antibodies also reduced *R.*
160 *delemar* ability to injure nasal epithelial cells by ~60%. As expected, anti-integrin $\beta 1$ antibodies had no effect

161 on *R. delemar*-mediated adhesion to, invasion and damage of nasal epithelial cells (**Fig. 2E**). In contrast, when
162 compared to isotype-matched control antibodies, the use of anti-integrin $\beta 1$ antibodies, and not anti-GRP78
163 antibodies, almost completely abolished the ability of *R. delemar* to invade alveolar epithelial cells (>95%
164 reduction in invasion) (**Fig 2F**). Similar to anti-GRP78 and nasal epithelial cells, anti-integrin $\beta 1$ antibodies had
165 no effect on the adherence of the fungus to alveolar epithelial cells (median adherence of 98%, 93% and 108%
166 for isotype-matched IgG, anti-GRP78 IgG, anti-integrin $\beta 1$ IgG, respectively, $P>0.1$). Finally, only anti-integrin
167 $\beta 1$ antibodies decreased the mold-mediated damage to alveolar epithelial cells by ~60% (**Fig. 2F**). Overall,
168 these results highlight that GRP78 and integrin $\beta 1$ act as major and specific receptors to *R. delemar* during
169 invasion and subsequent damage of nasal and alveolar epithelial cells, respectively.

170 We previously demonstrated the importance of *R. delemar* interacting with GRP78 by overexpressing
171 GRP78 on Chinese Hamster Ovarian cells (CHO) and showed increased *R. delemar*-mediated invasion and
172 damage of the transfected cells (14). To validate the importance of integrin $\beta 1$ as a receptor for *R. delemar*
173 during invasion of alveolar epithelial cells, we compared the ability of *R. delemar* to invade and damage GD25
174 fibroblast cell line which is generated from an integrin $\beta 1^{-/-}$ mouse, to $\beta 1$ AGD25 cell line made by transfecting
175 GD25 cells with mouse integrin $\beta 1$ cDNA (24). Despite the lack of difference in adhesion of *R. delemar* to
176 these two cell lines, the $\beta 1$ GD25 fibroblast cells expressing integrin $\beta 1$ was more susceptible to *R. delemar*-
177 mediated invasion and damage when compared to GD25 cells lacking integrin $\beta 1$ (an increase of ~ 600% for
178 invasion and 150% for damage of $\beta 1$ GD25 versus GD25 cells) (**Fig. 3A**). These data reaffirm the importance of
179 integrin $\beta 1$ as a host receptor for *R. delemar* during invasion and subsequent damage of alveolar epithelial cells.

180 For cell membrane proteins to act as host cell receptors they must be in close proximity to invading
181 fungal cells. Therefore, we used an indirect immunofluorescence assay to localize integrin $\alpha 3\beta 1$ on alveolar
182 epithelial cells during infection with *R. delemar* germlings. Both integrin $\alpha 3$ (stained with anti-integrin $\alpha 3$
183 antibody fluorescing green) and $\beta 1$ (stained with anti-integrin $\beta 1$ antibody fluorescing red) were expressed on
184 the surface of alveolar epithelial cells and coalesced on invading *R. delemar* germlings with an overlay images
185 showing clear intense yellow staining around the fungal cells (**Fig. 3B**).

186 We previously showed that the filamentous fungal pathogen *A. fumigatus* invades alveolar epithelial
187 cells through the fungus CalA protein binding to integrin $\alpha 5 \beta 1$ (25). Thus, to evaluate the function of integrin
188 $\alpha 5$ as a potential receptor for *R. delemar*, we repeated the indirect immunofluorescence assay using antibodies
189 targeting integrin $\beta 1$ and $\alpha 5$. As expected, integrin $\beta 1$ accumulated as a distinct ring-like formation around
190 endocytosed *R. delemar* germlings. In contrast, integrin $\alpha 5$ had a diffused staining without accumulation around
191 invading germlings (**Fig. S3**). Thus, these data strongly suggest that the receptor for *R. delemar* during invasion
192 of alveolar epithelial cells is likely to be integrin $\alpha 3 \beta 1$, rather than $\alpha 5 \beta 1$.

193 To confirm the identity of the alveolar epithelial cell receptor during Mucorales invasion, we incubated
194 the *R. delemar* germlings with A549 epithelial cells in the presence of specific monoclonal antibodies targeting
195 either integrin $\alpha 3$, $\alpha 5$, or $\beta 1$ separately and the two dimers of integrin $\alpha 3 \beta 1$, or $\alpha 5 \beta 1$. While all treatments
196 resulted in reduction of cellular invasion compared to the isotype-matched IgG antibodies (which did not block
197 invasion), there were differences in the extent of invasion inhibition. Specifically, targeting integrin $\beta 1$ caused
198 the greatest reduction in invasion with ~70% inhibition, while anti-integrin $\alpha 3$ and anti-integrin $\alpha 5$ antibodies
199 individually provided ~50% and 30% protection from invasion, respectively (**Fig. 3C**). Interestingly, targeting
200 both integrin $\alpha 3 \beta 1$ resulted in similar inhibition of *R. delemar* invasion of A549 cells when compared to
201 invasion inhibition provided by anti- $\beta 1$ antibody of ~70% and significantly more than the invasion inhibition
202 generated by anti- $\alpha 3$ antibody or anti- $\alpha 5 \beta 1$ (**Fig. 3C**). Collectively, these results show that integrin $\beta 1$ is the
203 major host receptor acting as a heterodimer with $\alpha 3$ during *R. delemar* invasion of alveolar epithelial cells and
204 blocking these receptors can reduce *R. delemar* virulence to alveolar epithelial cells *in vitro*.

205
206 **Integrin $\beta 1$ signaling is required for EGFR phosphorylation in alveolar epithelial cells during Mucorales**
207 **infection.** We recently reported EGFR acts as a receptor for *R. delemar* during invasion of alveolar epithelial
208 cells (20). However, the mechanism by which EGFR signaling is stimulated during infection was not identified.
209 We tested if integrin $\beta 1$ signaling played a role in stimulating EGFR activation during *R. delemar*-invasion, by
210 examining phosphorylation of the A549 cells' EGFR tyrosine residue 1068 in the presence of anti-integrin $\beta 1$

211 antibodies. Using immunoblotting assay, we determined that infection with *R. delemar* induces the EGFR
212 phosphorylation in A549 cells. When the *R. delemar*/A549 cell interaction was performed in the presence of
213 integrin $\beta 1$ antibodies, the phosphorylation of EGFR was abolished to the basal levels (**Fig. 4**). Thus, these
214 results are consistent with a model in which *R. delemar* interacts with integrin $\beta 1$ causing activation of EGFR.

215

216 ***R. delemar* cell surface proteins CotH3 and CotH7 are the fungal ligands to nasal and alveolar epithelial**
217 **cells, respectively.** Having identified the receptor on nasal and alveolar epithelial cells that interacts with *R.*
218 *delemar* germlings, we next sought to identify the fungal cell surface protein that binds to GRP78 and integrin
219 $\alpha 3\beta 1$. Far-Western blot analysis using recombinant human GRP78 followed by anti-GRP78 antibodies or
220 human integrin $\alpha 3\beta 1$ followed by anti-integrin $\alpha 3\beta 1$ antibodies identified the presence of prominent bands from
221 the supernatant of *R. delemar* regenerated protoplasts that bound to GRP78 (**Fig. 5A**) or integrin $\alpha 3\beta 1$ (**Fig.**
222 **6A**). LC-MS of the bands identified CotH3 and CotH7 as putative fungal ligands binding to GRP78 and integrin
223 $\alpha 3\beta 1$, respectively. We previously described that CotH3 is the fungal ligand to host GRP78 during interaction
224 of *R. delemar* with human umbilical vein endothelial cells (15, 26). Therefore, we used tools available for us to
225 determine the importance of CotH3 to *R. delemar* when interacting with nasal epithelial cells. We incubated
226 biotinylated nasal epithelial cell membrane proteins with the model yeast *Saccharomyces cerevisiae* harboring a
227 plasmid expressing CotH3 or *S. cerevisiae* expressing the empty plasmid as a negative control. The CotH3
228 expressing *S. cerevisiae* bound the 78-kDa protein of GRP78 as confirmed by Western blotting with anti-
229 GRP78 antibodies, whereas *S. cerevisiae* strain expressing empty plasmid did not (**Fig. 5B**). Next, we visualized
230 the interaction between the two host-fungal proteins by a proximity ligation assay (PLA). In this assay, non-
231 fluorescent primary antibodies (commercially available) raised in different species are allowed to recognize
232 GRP78 and CotH3 (using anti-CotH3 antibodies that we previously described (27)) on the host cells and
233 fungus, respectively. Secondary antibodies directed against the constant regions of the two primary antibodies
234 called PLA probes bind to the primary antibodies. The PLA probes fluoresce as a distinct bright spot only if the
235 two proteins of GRP78 and CotH3 are in close proximity. Indeed, nasal epithelial cell-*R. delemar* germling

236 interaction triggered the probe to fluoresce red (**Fig. 5C**). This fluorescence was located on germlings that
237 interacted with host cells stained with DAPI yielding a bright pink color. Therefore, *R. delemar* CotH3 interacts
238 with the GRP78 receptor on nasal epithelial cells leading to invasion and subsequent damage of host cells.

239 To investigate if the interactions of CotH3/GRP78 and CotH7/integrin $\alpha 3\beta 1$ result in mediating *R.*
240 *delemar* invasion and damage of nasal and alveolar epithelial cells, we specifically down regulated the
241 expression of CotH3 or CotH7 in *R. delemar* by RNAi. Individually targeting CotH3 and CotH7 by RNAi
242 resulted in generating *R. delemar* mutants that had ~90% (15) and 50% (**Fig. S4**) inhibition in these two genes,
243 respectively. Mutants were compared to the *R. delemar* strain transformed with an empty plasmid, in their
244 ability to invade and damage nasal and alveolar epithelial cells. Incubating nasal epithelial cells with an *R.*
245 *delemar* RNAi-suppressed CotH3 strain displayed >50% defect in invasion of and damage to nasal epithelial
246 cells when compared to *R. delemar* strain transformed with the empty plasmid. The inhibition of CotH3
247 expression had no effect on adherence of *R. delemar* to nasal epithelial cells (**Fig. 5D**), nor did it affect the
248 ability of *R. delemar* to interact with alveolar epithelial cells (**Fig. S5**). Therefore, CotH3 is a specific *R.*
249 *delemar* ligand that mediates invasion and subsequent damage to nasal epithelial cells..

250 We previously generated anti-CotH3 antibodies that blocked *R. delemar* mediated invasion of
251 endothelial cells. Therefore, we tested the ability of these antibodies to block *R. delemar*-mediated invasion of
252 and subsequent damage to nasal epithelial cells. Anti-CotH3 antibodies resulted in 60% and 75% reduction in
253 the ability of *R. delemar* to invade and damage nasal epithelial cells when compared to isotype-matched control
254 IgG, respectively (**Fig. 5E**). These results further confirm the importance of CotH3 protein in *R. delemar*
255 interacting with nasal epithelial cells *in vitro*. Interestingly, anti-CotH3 antibodies showed reduction in *R.*
256 *delemar*-mediated invasion to alveolar cells when compared to isotype-matched IgG (**Fig. S5B**).

257 Down regulation of CotH7 expression resulted in a statistically significant reduction (30% reduction) in
258 *R. delemar*-mediated damage of alveolar epithelial cells (**Fig. 6B**). Similar to the outcome of RNAi CotH3
259 mutant interacting with alveolar epithelial cells, down regulation of the CotH7 expression had no effect on *R.*

260 *delemar* interacting with nasal epithelial cells (**Fig. S7**). Therefore, interactions of *R. delemar* with alveolar
261 epithelial cells are mainly driven by CotH7 binding to integrin $\alpha3\beta1$.
262
263 **DKA host factors enhance *R. delemar*-mediate damage of nasal but not alveolar epithelial cells.** We have
264 previously shown that endothelial cell GRP78 and Mucorales CotH3 are overexpressed in physiological
265 conditions found in DKA patients such as hyperglycemia, elevated available serum iron and high concentrations
266 of ketone bodies, leading to enhanced invasion and damage of endothelial cells (14, 15, 26). Because we found
267 that *R. delemar* uses similar mechanism to interact with nasal epithelial cells, we reasoned that upregulation of
268 GRP78 on nasal epithelial cells might lead to entrapment of inhaled spores in the nasal cavity of DKA patients
269 leading to rhino-orbital disease rather than pulmonary infection. To test this hypothesis, we measured the effect
270 of physiologically elevated concentrations of glucose, iron and β -hydroxy butyrate (BHB, as a representation
271 for ketone bodies) on the GRP78 expression of nasal epithelial cells and subsequent interactions with *R.*
272 *delemar*. The use of elevated concentrations of glucose (4 or 8 mg/ml), iron (15-50 μ M of FeCl_3), or BHB (5-10
273 mM) resulted in ~2-6 fold increase in the surface expression of GRP78 on nasal epithelial cells when compared
274 to normal concentrations of 1 mg/ml glucose, 0 μ M iron, or 0 mM BHB (**Fig. 7A**). This enhanced expression of
275 GRP78 coincided with increased ability of *R. delemar* to invade (**Fig. 7B**) and subsequently damage (**Fig. 7C**)
276 nasal epithelial cells (~150%-170% increase in invasion and 120%-170% in nasal epithelial cells damage vs.
277 normal concentration of the effector). Conversely, the same elevated concentrations of glucose, iron and BHB
278 had no effect on the surface expression of integrin $\beta1$ of alveolar epithelial cells (**Fig. 8A**) nor did it result in
279 enhanced *R. delemar*-mediated invasion (with the exception of 8 mg/ml glucose that caused a modest increase
280 in invasion of 25% versus 1 mg/ml glucose) (**Fig. 8B**). Surprisingly, and in general, elevated concentrations of
281 glucose, iron, or BHB resulted in 40-50% protection of alveolar epithelial cells from *R. delemar*-mediated
282 injury (**Fig. 8C**). Collectively, these data suggest that nasal epithelial cells are more prone to *R. delemar*--
283 mediated invasion and injury than alveolar epithelial cells when exposed to DKA host factors, and likely

284 explain at least, in part, the reason why DKA patients predominantly suffer from rhinoorbital rather than
285 pulmonary mucormycosis.

286
287 **Anti-Integrin β 1 antibodies protect neutropenic mice from pulmonary mucormycosis.** We have previously
288 shown that GRP78 can be targeted for treating experimental mucormycosis (14). To examine the potential of
289 targeting integrins in treating pulmonary mucormycosis, we infected neutropenic mice intratracheally with *R.*
290 *delemar* spores, and treated them one day after infection with either an isotype-matched IgG or anti-integrin β 1
291 polyclonal IgG. While mice treated with the isotype-matched IgG had a median survival time of 11 days and
292 100% mortality by day 15 post infection, mice treated with the anti-integrin β 1 IgG had an improved median
293 survival time of 16 days and 30% of the mice survived by day 21 post infection when the experiment was
294 terminated (**Fig. 9**). The surviving mice appeared healthy, and lungs and brains (primary and secondary target
295 organs in this model (28)) harvested from the surviving mice had no residual infection as determined by lack of
296 fungal growth from harvest organs when cultured on potato dextrose agar (PDA) plates. Thus, these data
297 suggest that targeting integrin β 1 should be explored to serve as a promising novel therapeutic option against
298 pulmonary mucormycosis.

302 **Discussion**

303 Rhinorbital/cerebral and pulmonary infections are the two most common manifestations of lethal
304 mucormycosis (29). Despite acquiring the infection through inhaled spores, these two forms of disease
305 manifestations are determined by host underlying predisposing factors. Specifically, patients with DKA appear
306 to be more likely than other susceptible hosts to have rhinorbital/cerebral infection, while pulmonary
307 mucormycosis afflicts neutropenic/leukemic hosts (12, 30, 31). Since the reason for this disparity is unknown
308 (32), we questioned if Mucorales recognize host receptors expressed uniquely in distinct niches, especially in
309 response to specific host environmental conditions. We previously found that the fungal cell surface CotH3
310 protein, a unique invasin to Mucorales fungi, binds to mammalian GRP78 when infecting and damaging
311 umbilical vein endothelial cells (14, 15). Importantly, the expression of GRP78 host receptor and CotH3 fungal
312 ligand increases several folds under physiological conditions present in the DKA patients such as
313 hyperglycemia, elevated iron, and ketoacidosis leading to enhanced fungal invasion, subsequent damage of
314 endothelial cells and disease progression (26). Similar to these findings, we present multiple evidences by using
315 affinity purification, specific antibody blocking, colocalization and gene downregulation studies, to show that *R.*
316 *delemar* invades and damages nasal epithelial cells by CotH3 interacting with GRP78. As expected, DKA
317 conditions of hyperglycemia, elevated iron, and ketoacidosis resulted in upregulation of GRP78 of nasal
318 epithelial cells causing enhanced fungal invasion. Therefore, in patients with DKA, inhaled Mucorales spores
319 are likely trapped in the nasal milieu by the interaction of upregulated expression of GRP78/CotH3 resulting in
320 rhinorbital mucormycosis (**Fig. 10A**). The highly angioinvasive *R. delemar* can eventually spread from the
321 damaged nasal epithelial cells into surrounding tissue vasculature by continuing to interact with GRP78 on
322 endothelial cells (15, 26). In contrast, by using similar approaches we show that the integrin $\alpha 3\beta 1$ is the receptor
323 for *R. delemar* on alveolar epithelial cells which activated EGFR resulting in invasion and pulmonary infection
324 (**Fig. 10B**). However, hyperglycemia, elevated iron, and ketoacidosis, as seen in DKA patients did not increase
325 integrin $\alpha 3\beta 1$ expression on alveolar epithelial cells. In fact, through an unexplained mechanism(s), elevated
326 physiological concentrations of glucose, iron and BHB protected A549 cells from invasion and subsequent

327 damage by *R. delemar*. The protection of alveolar epithelial cells from *R. delemar*-mediated invasion and
328 subsequent damage when exposed to elevated glucose, iron, or BHB, likely to provide further explanation on
329 why DKA patients rarely develop pulmonary disease. Future studies will investigate the mechanism by which
330 DKA host factors protect alveolar epithelial cells from *R. delemar* –mediated invasion and damage.

331 One of the intriguing results is the difference of susceptibility of nasal and alveolar epithelial cells to *R.*
332 *delemar*-mediated damage despite equally being susceptible to fungal invasion. Specifically, nasal epithelial
333 cells were more susceptible to fungal damage when compared to alveolar epithelial cells (**Fig. 1**). We
334 previously reported on the role of *R. delemar* toxins in mediating damage to host cells (33). It is possible that
335 the two cell types have distinct susceptibility and/or induce different levels and/or types of these toxins.
336 Alternatively, binding to distinct receptors is likely to induce specific signal transductions pathways that might
337 explain the differences in host cell death pattern. These possibilities are the topic of active investigation in our
338 laboratory.

339 We previously reported on the CotH gene family which is uniquely and universally present in Mucorales
340 fungi and required for mucormycosis pathogenesis (15, 22). Specifically, CotH3 mediates invasion of
341 endothelial cells by binding to GRP78 (15, 26). *R. delemar* also uses CotH3 to invade nasal epithelial cells via
342 binding to GRP78. However, in lung tissues where integrins are highly expressed
343 (<https://www.ncbi.nlm.nih.gov/gene/3675>), CotH7 appears to be the major *R. delemar* ligand mediating binding
344 to integrin $\alpha 3\beta 1$ of alveolar epithelial cells. Although CotH2 and CotH3 proteins are closely related, CotH7 is
345 distantly related with ~ 50% amino acid identity to CotH3 (**Fig. S7**). It is noted that CotH2, CotH3, and CotH7
346 are among the most expressed genes in the entire genome of two clinical isolates (*R. delemar* 99-880 and *R.*
347 *oryzae* 99-892) and their expression is not induced by alveolar epithelial cells (22). This non-induced high
348 expression and the presence of altered protein family members is likely necessary for the organism to
349 successfully infect host niches in which invasion of tissues is dictated by the presence of different receptors.
350 However, in both nasal and alveolar epithelial cells, antibody blocking studies targeting the receptors or the

351 ligands did not completely block *R. delemar*-mediated adhesion, invasion or damage of host cells. Thus, other
352 host receptors/fungal ligands are likely to be involved in these interactions.

353 We found that anti-CotH3 antibodies, but not reduction of CotH3 expression by RNAi, were able to
354 block invasion, and to a lesser extent, adherence of *R. delemar* to alveolar epithelial cells (**Fig S5**). It is noted,
355 that the antibodies were generated against a peptide of CotH3 (MGQTNDGAYRDPTDNN (27)) that is ~70%
356 conserved in CotH7 protein (Fig S8), whereas the inhibition of CotH3 expression by RNAi resulted in ~ 80%
357 gene silencing (15).

358 Integrins are a family of adhesion receptors consisting of α and β heterodimer transmembrane subunits
359 that are specialized in binding cells to the extracellular matrix (23). They can also function as receptors for
360 extracellular ligands and transduce bidirectional signals into and outside the cell using effector proteins (34, 35).
361 One of such pathways is the ability of integrins to cooperate with EGFR leading to synergy in cell proliferation,
362 cell survival, and cell migration (36). We recently reported on the use of an unbiased survey of the host
363 transcriptional response during early stages of *R. delemar* infection in a murine model of pulmonary
364 mucormycosis as well as an *in vitro* A549 cell infection model by using transcriptome analysis sequencing.
365 RNA-seq data showed an activation of the host's EGFR by an unknown mechanism (20). Furthermore, an
366 FDA-approved inhibitor of EGFR, gefitinib, successfully inhibited alveolar epithelial cell invasion by *R.*
367 *delemar in vitro* and ameliorate experimental murine pulmonary mucormycosis (20). Our data highly suggests
368 that activation of the EGFR occurs by binding of the fungus to integrin $\beta 1$ (**Fig. 10B**). Specifically, the use of
369 anti-integrin $\beta 1$ antibody prevents the *R. delemar*-induced activation of EGFR.

370 We previously reported on protecting DKA mice from mucormycosis by using antibodies targeting
371 GRP78/CotH3 interactions (14, 15, 27). In these studies, mice were partially protected when the antibodies
372 were introduced alone and maximal protection occurred when anti-CotH3 antibodies were combined with
373 antifungal agents (27), indicating the potential translational benefit of this therapeutic approach. In this study,
374 we also demonstrated partial but highly significant protection against pulmonary mucormycosis when a single
375 administration of anti-integrin $\beta 1$ is used. This antibody dose translates into ~ 4.0 mg/kg, which is within the

376 antibody doses currently in clinical practice of 1-15 mg/kg, thereby emphasizing the clinical applicability of this
377 approach. One caveat of an immunotherapeutic approach targeting host cell receptors such as integrins or
378 GRP78 is the potential host toxicity. However, it is prudent to point that targets such as GRP78, integrins, or
379 EGFR are the subject of developing and/or developed therapeutic strategies against cancer (36, 37). One
380 advantage of developing therapies targeting integrins would be the possibility of using the developed therapy to
381 treat aspergillosis since we showed that integrin $\beta 1$ was also identified as a host receptor on A549 alveolar
382 epithelial cells when interaction with *A. fumigatus* cell surface protein CalA (25). *A. fumigatus* CalA
383 specifically interacts with integrin $\alpha 5\beta 1$ subunit, rather than integrin $\alpha 3\beta 1$, the predominant receptor for *R.*
384 *delemar*. However, blocking of integrin $\alpha 5$ or $\alpha 5\beta 1$ also resulted in a modest yet detectable decrease in
385 *Rhizopus* invasion of alveolar epithelial cells, indicating that the $\alpha 5$ subunit may play a minor role in fungal
386 interactions. Therefore, a therapy that targets both infections would have to focus on targeting integrin $\beta 1$.
387 Finally, nasal and/or alveolar epithelial cell interactions are early steps of the disease, and any potential therapy
388 targeting these interactions are likely to be more successful if initiated early on, preferably with antifungal
389 therapy to block invasion and enhance fungal clearance. Unfortunately, diagnosis of mucormycosis often occurs
390 in late-stage disease and currently reliant on histopathology or non-specific radiological methods (38).
391 However, early results of several methods reliant on molecular diagnosis (including those targeting CotH genes
392 (39-42)) and serology (targeting mannans (43)) are encouraging and likely to help in implementing early
393 therapy.

394 To summarize, the unique susceptibility of DKA subjects to rhinocerebral mucormycosis is likely due to
395 specific interaction between nasal epithelial cell GRP78 and fungal CotH3, the expression of which increase in
396 the presence of environmental factors present in DKA, which results in trapping inhaled spores in the nasal
397 cavity. In contrast, pulmonary mucormycosis is initiated via interaction of inhaled spores expressing CotH7
398 with integrin $\alpha 3\beta 1$ receptor which activates EGFR to induce fungal invasion of host cells. These results add to
399 our previously published line of evidence on the pathogenesis of mucormycosis in different hosts, and provide
400 groundwork for the development of therapeutic interventions against lethal drug-resistant mucormycosis.

401 **Methods**

402 ***R. delemar* and culture conditions**

403 A variety of clinical Mucorales isolates was used in this study. *R. delemar* 99-880 (brain isolate from a patient
404 with rhinocerebral mucormycosis), *R. oryzae* 99-892 (isolated from a patient with pulmonary mucromycosis)
405 and *Mucor circinelloides* 131 were obtained from the Fungus Testing laboratories at University of Texas Health
406 Science Center at San Antonio (UTHSCSA), Texas. *Lichtheimia corymbifera* strain 008-0490 and *Rhizomucor*
407 were collected from patients enrolled in the The Deferasirox-AmBisome Therapy for Mucormycosis study
408 (DEFEAT Mucormycosis) (44), *Cunninghamella bertholletiae* 182 is a clinical isolate obtained from Dr.
409 Thomas Walsh, (NIH, Bethesda, Maryland, USA). *Saccharomyces cerevisiae* ATCC 62956 (LL-20), its his3 Δ
410 and leu Δ , was constructed by L. Lau (University of Illinois at Chicago). *S. cerevisiae* expressing *R. delemar*
411 CotH3 protein driven by the galactose inducible promoter (15) was utilized to confirm the candidate ligand for
412 the nasal epithelial cells. Mucorales were grown on PDA plates (BD Biosciences — Diagnostic Systems) plates
413 for 3–5 days at 37°C, while *S. cerevisiae* was grown on synthetic dextrose minimal medium (SD) for 3-5 days.
414 All incubations were done at 37°C. To induce the expression of CotH3 in *S. cerevisiae*, the yeast cells were
415 grown in synthetic galactose minimal medium (SG) at 37°C for 16 hours. The sporangiospores were collected
416 in endotoxin-free Dulbecco's phosphate buffered saline (PBS) containing 0.01% Tween 80 for Mucorales,
417 washed with PBS, and counted with a hemocytometer to prepare the final inoculum. For *S. cerevisiae*, cells
418 were centrifuged, and washed with PBS and counted as above.

419 To form germlings, spores were incubated in Kaighn's Modification of Ham's F-12 Medium (F-12K
420 from the American Type Culture Collection [ATCC]) medium at 37°C with shaking for 1–3 hours based on the
421 assay under study. Germlings were washed twice with F-12 Medium for all assays used, except in experiments
422 involving isolation of the epithelial cell receptor, for which the germlings were washed twice with PBS (plus
423 Ca⁺⁺ and Mg⁺⁺).

424

425 **Host cells**

426 Nasal epithelial cells (CCL-30) were obtained from ATCC and cultured in Eagle's Minimum Essential Medium
427 (EMEM) supplemented with 10% fetal bovine serum and penicillin-streptomycin. Homo sapiens alveolar
428 epithelial cells (A549 cells) procured from ATCC were obtained from a 58-year-old male Caucasian patient
429 with carcinoma. They were propagated in F-12 Medium developed for alveolar A549 epithelial cells. The GD25
430 and β 1AGD25 cell lines were obtained from Dr. Deane F. Mosher, University of Wisconsin-Madison. The cells
431 were cultured to confluency in Falcon Tissue Culture Treated Flasks (75cm²) at 37°C with 5% CO₂.

433 **Invasion of *R. delemar* to epithelial cells**

434 The number of organisms invading epithelial cells was determined using a modification of our previously
435 described differential fluorescence assay (45). Briefly, 12-mm glass coverslips in 24-well cell culture plate were
436 coated with fibronectin for at least 4 hours and seeded with epithelial cells until confluency. After washing
437 twice with prewarmed Hank's Balanced Salt Solution (HBSS, Irvine Scientific) , the cells were then infected
438 with 2.5×10^5 cells of *R. delemar* in F-12K medium that had been germinated for 2 hours. Following incubation
439 for 3 hours, the cells were fixed in 3% paraformaldehyde and were stained for 1 hour with 1% Uvitex
440 (Polysciences), which specifically binds to the chitin of the fungal cell wall. After washing 5 times with PBS,
441 the coverslips were mounted on a glass slide with a drop of ProLong Gold antifade reagent and sealed with nail
442 polish. The total number of cell-associated organisms (i.e., germlings adhering to monolayer) was determined
443 by phase-contrast microscopy. The same field was examined by epifluorescence microscopy, and the number of
444 uninternalized germlings (which were brightly fluorescent) was determined. The number of endocytosed
445 organisms was calculated by subtracting the number of fluorescent organisms from the total number of visible
446 organisms. At least 100 organisms were counted in 20 different fields on each slide. Two slides per arm were
447 used for each experiment, and the experiment was performed in triplicate on different days.

449 ***R. delemar* –induced epithelial cell damage**

450 Host cell damage was quantified by using a chromium (^{51}Cr)-release assay (46). Briefly, epithelial cells grown
451 in 24-well tissue culture plates were incubated with 1 μCi per well of $\text{Na}_2^{51}\text{CrO}_4$ (ICN) in EMEM or F12-K
452 medium (for nasal or alveolar cells) for 16 hours. On the day of the experiment, the unincorporated ^{51}Cr was
453 aspirated, and the wells were washed twice with warmed HBSS. Cells were infected with 2.5×10^5 spores
454 suspended in 1 ml in EMEM or F-12K. Spontaneous ^{51}Cr -release was determined by incubating epithelial cells
455 in EMEM or F-12K medium without *R. delemar*. After 30 hours of incubation of spores with nasal cells, or 48
456 hours for alveolar cells, 50% of the medium was aspirated from each well and transferred to glass tubes.
457 Approximately 500 μl of 6 N NaOH was added to each well, incubated for 15 min, and the media transferred
458 from the wells to a glass tube. Subsequently each well was rinsed with 500 μl of RadiacWash (Biodex), and
459 transfer to the same tube. The amount of ^{51}Cr in the tubes was determined by gamma counting. The total
460 amount of ^{51}Cr incorporated by epithelial cells in each well equaled the sum of radioactive counts per minute of
461 the aspirated medium plus the radioactive counts of the corresponding cells. After the data were corrected for
462 variations in the amount of tracer incorporated in each well, the percentage of specific epithelial cell release of
463 ^{51}Cr was calculated by the following formula: $[(\text{experimental release} \times 2) - (\text{spontaneous release} \times 2)] / [\text{total}$
464 $\text{incorporation} - (\text{spontaneous release} \times 2)]$. Each experimental condition was tested at least in triplicate and the
465 experiment repeated at least once.

466 For Ab-mediated blocking of adherence, invasion or damage caused by *R. delemar*, the assays were carried out
467 as above except that epithelial cells were incubated with the respective antibodies [50 $\mu\text{g}/\text{ml}$ anti-GRP78 or 5
468 $\mu\text{g}/\text{ml}$ anti-integrin $\beta 1$ or integrin $\alpha 3\beta 1$ Ab or Anti-IgG (as an isotype matching control)] for 1 hour prior to
469 addition of *R. delemar* germlings.

471 **Effect of acidosis, iron, glucose or β -hydroxy butyrate on *R. delemar* –epithelial cell interactions**

472 Studies were performed to investigate the effect of glucose, iron or BHB on epithelial cell GRP78 or integrin
473 expression levels, and to test their impact on subsequent interactions of epithelial cells with *R. delemar*
474 germlings. Epithelial cells were grown in EMEM or F-12K media containing varying concentrations of FeCl_3 ,

475 glucose or BHB for 5 hours. GRP78 or integrin expression, invasion, and damage assays were conducted as
476 mentioned in the previous section.

478 **Extraction of epithelial cell membrane proteins**

479 Epithelial cell membrane proteins were extracted according to the method of Isberg and Leong (21). Briefly,
480 epithelial cells grown to confluency in 20 flasks of 75 cm² were split into ten tissue culture dishes 150 mm x 25
481 mm and incubated at 37°C in 5% CO₂ until they reached confluency (normally 5-7 days). The cells were
482 washed two times with 12 ml warm PBS containing Ca⁺⁺ and Mg⁺⁺ (PBS-CM) prior to incubating them with
483 0.5 mg/ml EZ-Link sulfo-NHS-LS-Biotin (Pierce) (12 minutes in 5% CO₂ at 37°C). Subsequently, the cells
484 were then rinsed extensively with cold PBS-CM and scraped from the tissue culture dishes. The epithelial cells
485 were collected by centrifugation at 500 g for 5 minutes at 4°C and then lysed by incubation for 20 minutes on
486 ice in PBS-CM containing 5.8% n-octyl-β-d-glucopyranoside (Fisher) and protease inhibitor cocktail solution
487 (Fisher). The cell debris was removed by centrifugation at 5,000 g for 5 minutes at 4°C. The supernatant was
488 collected and centrifuged at 100,000 g for 1 hour at 4°C. The concentration of the epithelial cell proteins in the
489 resulting supernatant was determined using the Bradford method (Bio-Rad).

491 **Isolation of epithelial cell receptors that bind to Mucorales**

492 Live Mucorales spores (1×10^8) or an equivalent volume of 1–3 hours germlings (approximately 1×10^8 cells)
493 were incubated for 1 hour on ice with 250 μg of biotin-labeled epithelial cell surface proteins in PBS-CM plus
494 1.5% n-octyl-β-d-glucopyranoside and protease inhibitor cocktail. The unbound epithelial cell proteins were
495 washed away by 5 rinses with this buffer. The epithelial cell proteins that remained bound to the fungal cells
496 were eluted twice with 6 M urea (Sigma). The proteins were then separated on 10% SDS-PAGE and transferred
497 to immun-Blot PVDF Membrane (BIO-RAD). The membrane was then treated with Western Blocking Reagent
498 (Roche) and probed with anti-biotin, HRP conjugated linked antibody (Cell Signaling). After incubation with
499 SuperSignal West Dura Extended Duration Substrate (Pierce), the signals were detected using a CCD camera.

To identify epithelial cell proteins that bound to Mucorales, we incubated epithelial cell membrane proteins with *R. delemar* germlings as above. The eluted proteins were separated by SDS-PAGE, and the gel was stained with Instant Blue Stain (Fisher). The major two bands at approximately 75 and 130 kDa (from alveolar and nasal cells) were excised and micro sequenced using MALDI-TOF MS/MS (The Lundquist Institute Core Facility).

To confirm the identity of GRP78 and integrin $\alpha 3\beta 1$, epithelial cells membrane proteins that bound to *R. delemar* were separated on an SDS-polyacrylamide gel and transferred to PVDF-plus membranes. Membranes were probed with a rabbit anti-GRP78 antibody (Abcam), followed by HRP-conjugated goat anti-rabbit IgG (Pierce) as a secondary Ab (for nasal cells) and rabbit anti-integrin $\alpha 3\beta 1$ (Abcam), followed by HRP-conjugated goat anti-rabbit IgG (Pierce). After incubation with SuperSignal West Dura Extended Duration Substrate (Pierce), the signals were detected using enhanced chemiluminescence and imaged with a C400 (Azure Biosystems) digital imager.

Immunoblot of EGFR phosphorylation *in vitro*

A549 cells in 24-well tissue culture plates were incubated in F-12K tissue culture medium supplemented with fetal bovine serum to a final concentration of 10%. Prior to infection, the A549 cells were serum starved for 120 minutes. Spores of *R. delemar* was incubated in RPMI for 60 minutes at 37°C, washed, and suspended in F-12K medium. A549 cells were infected for 3 hours with a multiplicity of infection (MOI) of 5. Next, the cells were rinsed with cold HBSS containing protease and phosphatase inhibitors and removed from the plate with a cell scraper. After collecting the cells by centrifugation, they were boiled in 2x SDS sample buffer. The lysates were separated by SDS-PAGE, and Y1068 EGFR phosphorylation was detected with a phospho-specific antibody (Cell Signaling). The blots were then stripped, and total protein levels was detected by immunoblotting with appropriate antibodies against EGFR (Cell Signaling). The immunoblots were developed using enhanced chemiluminescence and imaged with a C400 (Azure Biosystems) digital imager.

525 **Colocalization of GRP78 and integrin $\alpha 3\beta 1$ with phagocytosed *R. delemar* germlings**

526 We used a modification of our previously described method (14). Confluent epithelial cells on a 12-mm-
527 diameter glass coverslip were infected with 2.5×10^5 cells/ml *R. delemar* cells in EMEM or F12-K mediums
528 that had been pregerminated for 2 hours. After 3 hours incubation at 37°C, the cells were gently washed twice
529 with HBSS to remove unbound organisms, and then fixed with 3% paraformaldehyde for 15 min.

530 For *R. delemar* interaction with nasal cells, a proximity ligation assay technique (PLA, Sigma Aldrich)
531 was performed. For the PLA assay, two primary antibodies raised in different species are used to detect two
532 unique protein targets. A pair of oligonucleotide-labeled secondary antibodies (PLA probes) then binds to the
533 primary antibodies. Hybridizing connector oligos join the PLA probes only if they are in close proximity to
534 each other, allowing for up to 1000-fold amplified signal tethered to the PLA probe, resulting in localization of
535 the signal. This is visualized and quantified as discrete spots (PLA signals) by microscopy image analysis.
536 Thus, two different antibodies - a mouse anti-GRP78 IgG was used to stain paraformaldehyde-fixed nasal cells,
537 while anti-rabbit IgG against CotH3 was used to label *R. delemar*. Interaction between the two cell-surface
538 proteins were carried out according to the kit instructions and visualized by confocal microscopy.

539 For alveolar epithelial cell-*R. delemar* interaction, the formaldehyde-fixed epithelial cell-spore mixture
540 were incubated with 1% BSA for 1 h (blocking step). Next, cells were incubated with antibodies against
541 integrin $\alpha 3$ or integrin $\beta 1$ (eBioscience, Santa Cruz), followed by the appropriate secondary antibodies labeled
542 with either Alexa Fluor 488 or Alexa Fluor 568 (Thermo Fisher Scientific). After washing, the coverslip was
543 mounted on a glass slide with a drop of ProLong Gold antifade reagent (Molecular Probes, Invitrogen) and
544 viewed by confocal microscopy. The final confocal images were produced by combining optical sections taken
545 through the z axis.

546 **Protoplast formation and collection of *R. delemar* cell wall material**

547 To identify the *R. delemar* ligand that binds to epithelial cell GRP78, we collected cell wall material from
548 supernatants of protoplasts of *R. delemar* germlings. Briefly, *R. delemar* spores (6×10^6) were germinated in
549

550 YPD medium for 3 hours at 37°C. Germinated cells were collected by centrifugation at 900 g, washed twice
551 with 0.5 M sorbitol, and then resuspended in 0.5 M sorbitol in sodium phosphate buffer (pH 6.4). Protoplasting
552 solution consisting of 0.25 mg/ml lysing enzymes (Sigma-Aldrich), 0.15 mg/ml chitinase (Sigma-Aldrich), and
553 0.01 mg/ml chitosinase (produced from *Bacillus circulans*) was added to the germinated spores and incubated
554 with gentle shaking at 30°C for 2 hours. Protoplasts were collected by centrifugation for 5 minutes at 200 g at
555 4°C, washed twice with 0.5 M sorbitol, and resuspended in the same buffer. Incubating protoplasts in the
556 presence of the osmotic stabilizer sorbitol enables regeneration of the cell wall, and during regeneration, cell
557 wall constituents are released into the supernatant (47-49), protoplasts were pelleted, and the supernatant was
558 sterilized by filtration (0.22- μ m filters) in the presence of protease inhibitors (Pierce). The supernatant was
559 concentrated, and protein concentration was measured using the Bradford method (BioRad). Negative control
560 samples were processed similarly, with the exception of the absence of protoplasts. Thus, far-western blot
561 analysis using recombinant human GRP78 and anti-GRP78 antibodies was done to identify *R.delemar* ligand.

562

563 ***In vivo* virulence studies**

564 For survival studies, equal numbers of male and female ICR mice (≥ 20 g) were purchased from Envigo and
565 housed in groups of 5 each. Mice were immunosuppressed with cyclophosphamide (200 mg/kg i.p.) and
566 cortisone acetate (500 mg/kg s.c.) on day -2, +3, and +8. Mice were infected with 2.5×10^5 in 25 μ l *R. delemar*
567 spores intratracheally. To confirm the inoculum, 3 mice were sacrificed immediately after inoculation, their
568 lungs were homogenized in PBS and quantitatively cultured on PDA plates containing 0.1% triton, and colonies
569 were counted after a 24-hour incubation period at 37°C. Mice were treated with a single dose of 100 μ g (i.p.)
570 anti- β 1 integrin antibody administrated 24 h post infection. Placebo mice received 100 μ g of isotype-matched
571 IgG. Mouse survival was monitored for 21 days, and any moribund mice were euthanized. Results were plotted
572 using Log-rank (Mantel-Cox) Test.

573

574 **Study approval.** All procedures involving mice were approved by the IACUC of The Lundquist Institute for
575 Biomedical Innovations at Harbor-UCLA Medical Center, according to the NIH guidelines for animal housing
576 and care. Human endothelial cell collection was approved by the IRB of The Lundquist Institute for Biomedical
577 Innovations at Harbor-UCLA Medical Center. Because umbilical cords are collected without donor identifiers,
578 the IRB considers them medical waste not subject to informed consent.

579

580 **Statistical analysis**

581 Differences in GRP78 or integrin β 1 expression and fungi–epithelial cell interactions were compared by the
582 nonparametric Mann-Whitney test. In the survival study, the nonparametric log-rank test was used to determine
583 differences between isotype IgG control and Ant-integrin β 1 Ab. Comparisons with *P* values < 0.05 were
584 considered significant.

585

586 **Acknowledgments**

587 This work was supported by a Public Health Service grant R01AI063503, R01AI141360 and SBIR
588 5R43AI138904 to ASI. MS is supported by R00DE026856, VMB by U19AI110820 and 358 R01AI141360, PU
589 by 1R21HD097480-01 and R01AI141794 and SGF by R01AI124566 and R01DE022600.

590 We would like to thank Drs. H. K. Choi, Davood Soleymani, and Helen Chun for their guidance and helpful
591 discussions.

592

593 **Competing interests**

594 A.S.I. owns shares in Vitalex Biosciences, a start-up company that is developing immunotherapies and
595 diagnostics for mucormycosis. The remaining authors declare no competing interests.

596

597 **References**

- 598 1. Ribes JA, Vanover-Sams CL, Baker DJ. 2000. Zygomycetes in human disease. *Clin Microbiol Rev*
599 13:236-301.
- 600 2. Spellberg B, Edwards J, Jr., Ibrahim A. 2005. Novel perspectives on mucormycosis: pathophysiology,
601 presentation, and management. *Clin Microbiol Rev* 18:556-69.
- 602 3. Chayakulkeeree M, Ghannoum MA, Perfect JR. 2006. Zygomycosis: the re-emerging fungal infection.
603 *Eur J Clin Microbiol Infect Dis* 25:215-29.
- 604 4. Ibrahim AS, Spellberg B, Walsh TJ, Kontoyiannis DP. 2012. Pathogenesis of mucormycosis. *Clin Infect*
605 *Dis* 54 Suppl 1:S16-22.
- 606 5. Kauffman CA. 2004. Zygomycosis: reemergence of an old pathogen. *Clin Infect Dis* 39:588-90.
- 607 6. Roden MM, Zaoutis TE, Buchanan WL, Knudsen TA, Sarkisova TA, Schaufele RL, Sein M, Sein T,
608 Chiou CC, Chu JH, Kontoyiannis DP, Walsh TJ. 2005. Epidemiology and outcome of zygomycosis: a
609 review of 929 reported cases. *Clin Infect Dis* 41:634-53.
- 610 7. Gleissner B, Schilling A, Anagnostopolous I, Siehl I, Thiel E. 2004. Improved outcome of zygomycosis
611 in patients with hematological diseases? *Leuk Lymphoma* 45:1351-60.
- 612 8. Ibrahim AS, Kontoyiannis DP. 2013. Update on mucormycosis pathogenesis. *Curr Opin Infect Dis*
613 26:508-15.
- 614 9. Andresen D, Donaldson A, Choo L, Knox A, Klaassen M, Ursic C, Vonthethoff L, Krilis S, Konecny P.
615 2005. Multifocal cutaneous mucormycosis complicating polymicrobial wound infections in a tsunami
616 survivor from Sri Lanka. *Lancet* 365:876-8.
- 617 10. Cocanour CS, Miller-Crotchet P, Reed RL, 2nd, Johnson PC, Fischer RP. 1992. Mucormycosis in
618 trauma patients. *J Trauma* 32:12-5.
- 619 11. Neblett Fanfair R, Benedict K, Bos J, Bennett SD, Lo YC, Adebajo T, Etienne K, Deak E, Derado G,
620 Shieh WJ, Drew C, Zaki S, Sugerman D, Gade L, Thompson EH, Sutton DA, Engelthaler DM, Schupp
621 JM, Brandt ME, Harris JR, Lockhart SR, Turabelidze G, Park BJ. 2012. Necrotizing cutaneous
622 mucormycosis after a tornado in Joplin, Missouri, in 2011. *N Engl J Med* 367:2214-25.
- 623 12. Kauffman CA, Malani AN. 2007. Zygomycosis: an emerging fungal infection with new options for
624 management. *Curr Infect Dis Rep* 9:435-40.
- 625 13. Ferguson BJ. 2000. Mucormycosis of the nose and paranasal sinuses. *Otolaryngol Clin North Am*
626 33:349-65.
- 627 14. Liu M, Spellberg B, Phan QT, Fu Y, Fu Y, Lee AS, Edwards JE, Jr., Filler SG, Ibrahim AS. 2010. The
628 endothelial cell receptor GRP78 is required for mucormycosis pathogenesis in diabetic mice. *J Clin*
629 *Invest* 120:1914-24.

- 630 15. Gebremariam T, Liu M, Luo G, Bruno V, Phan QT, Waring AJ, Edwards JE, Jr., Filler SG, Yeaman
631 MR, Ibrahim AS. 2014. CotH3 mediates fungal invasion of host cells during mucormycosis. *J Clin*
632 *Invest* 124:237-50.
- 633 16. Ferguson BJ. 2000. Mucormycosis of the nose and paranasal sinuses. *Otolaryngologic Clinics of North*
634 *America* 33:349-365.
- 635 17. Chinen K, Tokuda Y, Sakamoto A, Fujioka Y. 2007. Fungal infections of the heart: a clinicopathologic
636 study of 50 autopsy cases. *Pathol Res Pract* 203:705-15.
- 637 18. Dhooria S, Agarwal R, Chakrabarti A. 2015. Mediastinitis and Bronchial Perforations Due to
638 Mucormycosis. *J Bronchology Interv Pulmonol* 22:338-42.
- 639 19. Kontoyiannis DP, Wessel VC, Bodey GP, Rolston KV. 2000. Zygomycosis in the 1990s in a tertiary-
640 care cancer center. *Clin Infect Dis* 30:851-6.
- 641 20. Watkins TN, Gebremariam T, Swidergall M, Shetty AC, Graf KT, Alqarihi A, Alkhazraji S, Alsaadi AI,
642 Edwards VL, Filler SG, Ibrahim AS, Bruno VM. 2018. Inhibition of EGFR Signaling Protects from
643 Mucormycosis. *MBio* 9.
- 644 21. Isberg RR, Leong JM. 1990. Multiple beta 1 chain integrins are receptors for invasins, a protein that
645 promotes bacterial penetration into mammalian cells. *Cell* 60:861-71.
- 646 22. Chibucos MC, Soliman S, Gebremariam T, Lee H, Daugherty S, Orvis J, Shetty AC, Crabtree J, Hazen
647 TH, Etienne KA, Kumari P, O'Connor TD, Rasko DA, Filler SG, Fraser CM, Lockhart SR, Skory CD,
648 Ibrahim AS, Bruno VM. 2016. An integrated genomic and transcriptomic survey of mucormycosis-
649 causing fungi. *Nat Commun* 7:12218.
- 650 23. Tsuji T. 2004. Physiological and Pathological Roles of $\alpha\beta 1$ Integrin. *The Journal of Membrane Biology*
651 200:115-132.
- 652 24. Wennerberg K, Lohikangas L, Gullberg D, Pfaff M, Johansson S, Fassler R. 1996. Beta 1 integrin-
653 dependent and -independent polymerization of fibronectin. *J Cell Biol* 132:227-38.
- 654 25. Liu H, Lee MJ, Solis NV, Phan QT, Swidergall M, Ralph B, Ibrahim AS, Sheppard DC, Filler SG. 2016.
655 *Aspergillus fumigatus* CalA binds to integrin $\alpha 5\beta 1$ and mediates host cell invasion. *Nat*
656 *Microbiol* 2:16211.
- 657 26. Gebremariam T, Lin L, Liu M, Kontoyiannis DP, French S, Edwards JE, Jr., Filler SG, Ibrahim AS.
658 2016. Bicarbonate correction of ketoacidosis alters host-pathogen interactions and alleviates
659 mucormycosis. *J Clin Invest* doi:10.1172/JCI82744.
- 660 27. Gebremariam T, Alkhazraji S, Soliman SSM, Gu Y, Jeon HH, Zhang L, French SW, Stevens DA,
661 Edwards JE, Filler SG, Uppuluri P, Ibrahim AS. 2019. Anti-CotH3 antibodies protect mice from

- 662 mucormycosis by prevention of invasion and augmenting opsonophagocytosis. *Science Advances*
663 5:eaaw1327.
- 664 28. Luo G, Gebremariam T, Lee H, French SW, Wiederhold NP, Patterson TF, Filler SG, Ibrahim AS. 2013.
665 Efficacy of liposomal amphotericin B and posaconazole in intratracheal models of murine
666 mucormycosis. *Antimicrob Agents Chemother* 57:3340-7.
- 667 29. Kwon-Chung KJ, Bennett JE. 1992. Mucormycosis, p 524-559, *Medical Mycology*. Lea & Febiger,
668 Philadelphia.
- 669 30. Spellberg B, Edwards Jr. J, Ibrahim A. 2005. Novel perspectives on mucormycosis: pathophysiology,
670 presentation, and management. *Clin Microbiol Rev* 18:556-69.
- 671 31. Sugar AM. 2005. Agents of Mucormycosis and Related Species, p 2973-2984. *In* Mandell GL, Bennett
672 JE, Dolin R (ed), *Principles and Practice of Infectious Diseases*, 6th ed, vol 2. Elsevier Churchill
673 Livingstone, Philadelphia, PA.
- 674 32. Jeong W, Keighley C, Wolfe R, Lee WL, Slavin MA, Kong DCM, Chen SC. 2019. The epidemiology
675 and clinical manifestations of mucormycosis: a systematic review and meta-analysis of case reports.
676 *Clin Microbiol Infect* 25:26-34.
- 677 33. Baldin C, Soliman S, Jeon HH, Gebremariam T, Skory CD, Edwards JEJ, Ibrahim AS (ed). 2018.
678 Optimization of the CRISPR/Cas9 system to manipulate gene function in *Rhizopus delemar*. Lisbon,
679 Portugal.
- 680 34. Hynes RO. 2002. Integrins: Bidirectional, Allosteric Signaling Machines. *Cell* 110:673-687.
- 681 35. Harburger DS, Calderwood DA. 2009. Integrin signalling at a glance. *Journal of cell science* 122:159-
682 163.
- 683 36. Desgrosellier JS, Cheresch DA. 2010. Integrins in cancer: biological implications and therapeutic
684 opportunities. *Nature reviews Cancer* 10:9-22.
- 685 37. Lee AS. 2014. Glucose-regulated proteins in cancer: molecular mechanisms and therapeutic potential.
686 *Nature reviews Cancer* 14:263-276.
- 687 38. Cornely OA, Alastruey-Izquierdo A, Arenz D, Chen SCA, Dannaoui E, Hochhegger B, Hoenigl M,
688 Jensen HE, Lagrou K, Lewis RE, Mellingshoff SC, Mer M, Pana ZD, Seidel D, Sheppard DC, Wahba R,
689 Akova M, Alanio A, Al-Hatmi AMS, Arikian-Akdagli S, Badali H, Ben-Ami R, Bonifaz A, Bretagne S,
690 Castagnola E, Chayakulkeeree M, Colombo AL, Corzo-León DE, Drgona L, Groll AH, Guinea J,
691 Heussel C-P, Ibrahim AS, Kanj SS, Klimko N, Lackner M, Lamothe F, Lanternier F, Lass-Floerl C, Lee
692 D-G, Lehrnbecher T, Lmimouni BE, Mares M, Maschmeyer G, Meis JF, Meletiadis J, Morrissey CO,
693 Nucci M, Oladele R, Pagano L, et al. Global guideline for the diagnosis and management of
694 mucormycosis: an initiative of the European Confederation of Medical Mycology in cooperation with

- 695 the Mycoses Study Group Education and Research Consortium. *The Lancet Infectious Diseases*
696 doi:10.1016/S1473-3099(19)30312-3.
- 697 39. Baldin C, Soliman SSM, Jeon HH, Alkhazraji S, Gebremariam T, Gu Y, Bruno VM, Cornely OA,
698 Leather HL, Sugrue MW, Wingard JR, Stevens DA, Edwards JE, Jr., Ibrahim AS. 2018. PCR-based
699 approach targeting *Mucorales* specific gene family for the diagnosis of mucormycosis. *J Clin Microbiol*
700 doi:10.1128/JCM.00746-18.
- 701 40. Kasai M, Harrington SM, Francesconi A, Petraitis V, Petraitiene R, Beveridge MG, Knudsen T,
702 Milanovich J, Cotton MP, Hughes J, Schaufele RL, Sein T, Bacher J, Murray PR, Kontoyiannis DP,
703 Walsh TJ. 2008. Detection of a molecular biomarker for zygomycetes by quantitative PCR assays of
704 plasma, bronchoalveolar lavage, and lung tissue in a rabbit model of experimental pulmonary
705 zygomycosis. *J Clin Microbiol* 46:3690-702.
- 706 41. Alanio A, Garcia-Hermoso D, Mercier-Delarue S, Lanternier F, Gits-Muselli M, Menotti J, Denis B,
707 Bergeron A, Legrand M, Lortholary O, Bretagne S, French Mycosis Study G. 2015. Molecular
708 identification of *Mucorales* in human tissues: contribution of PCR electrospray-ionization mass
709 spectrometry. *Clin Microbiol Infect* 21:594 e1-5.
- 710 42. Millon L, Herbrecht R, Grenouillet F, Morio F, Alanio A, Letscher-Bru V, Cassaing S, Chouaki T,
711 Kauffmann-Lacroix C, Poirier P, Toubas D, Augereau O, Rocchi S, Garcia-Hermoso D, Bretagne S.
712 2016. Early diagnosis and monitoring of mucormycosis by detection of circulating DNA in serum:
713 retrospective analysis of 44 cases collected through the French Surveillance Network of Invasive Fungal
714 Infections (RESSIF). *Clinical Microbiology and Infection* 22:810.e1-810.e8.
- 715 43. Burnham-Marusich AR, Hubbard B, Kvam AJ, Gates-Hollingsworth M, Green HR, Soukup E, Limper
716 AH, Kozel TR. 2018. Conservation of Mannan Synthesis in Fungi of the Zygomycota and Ascomycota
717 Reveals a Broad Diagnostic Target. *mSphere* 3:e00094-18.
- 718 44. Spellberg B, Ibrahim AS, Chin-Hong PV, Kontoyiannis DP, Morris MI, Perfect JR, Fredricks D, Brass
719 EP. 2012. The Deferasirox-AmBisome Therapy for Mucormycosis (DEFEAT Mucor) study: a
720 randomized, double-blinded, placebo-controlled trial. *J Antimicrob Chemother* 67:715-22.
- 721 45. Ibrahim AS, Filler SG, Alcouloumre MS, Kozel TR, Edwards JE, Jr., Ghannoum MA. 1995. Adherence
722 to and damage of endothelial cells by *Cryptococcus neoformans* in vitro: role of the capsule. *Infect*
723 *Immun* 63:4368-74.
- 724 46. Ibrahim AS, Gebremariam T, Liu M, Chamilos G, Kontoyiannis D, Mink R, Kwon-Chung KJ, Fu Y,
725 Skory CD, Edwards JE, Jr., Spellberg B. 2008. Bacterial endosymbiosis is widely present among
726 zygomycetes but does not contribute to the pathogenesis of mucormycosis. *J Infect Dis* 198:1083-90.

- 727 47. Michielse CB, Salim K, Ragas P, Ram AF, Kudla B, Jarry B, Punt PJ, van den Hondel CA. 2004.
728 Development of a system for integrative and stable transformation of the zygomycete *Rhizopus oryzae*
729 by *Agrobacterium*-mediated DNA transfer. *Mol Genet Genomics* 271:499-510.
- 730 48. Pitarch A, Jimenez A, Nombela C, Gil C. 2006. Decoding serological response to *Candida* cell wall
731 immunome into novel diagnostic, prognostic, and therapeutic candidates for systemic candidiasis by
732 proteomic and bioinformatic analyses. *Mol Cell Proteomics* 5:79-96.
- 733 49. Pitarch A, Pardo M, Jimenez A, Pla J, Gil C, Sanchez M, Nombela C. 1999. Two-dimensional gel
734 electrophoresis as analytical tool for identifying *Candida albicans* immunogenic proteins.
735 *Electrophoresis* 20:1001-10.

736

737

738 **Figure legends.**

739 **Fig. 1. *R. delemar*-mediated invasion and damage of nasal and alveolar epithelial cells.** *R. delemar* invasion
740 of nasal (A) or alveolar (B) epithelial cells was determined using differential fluorescent assay by staining with
741 1% Uvitex for 1 hour, while damage assay was performed using ^{51}Cr release method. *** $P < 0.0001$ and ** P
742 < 0.001 compared to the first time point in each panel. Data presented as median \pm interquartile range from 3
743 independent experiments.

744

745 **Fig. 2. GRP78 is a nasal epithelial cell receptor, while integrin $\alpha 3\beta 1$ is an alveolar epithelial cell receptor**
746 **during Mucorales interaction.** Biotinylated nasal (A) or alveolar (B) epithelial cells were incubated with *R.*
747 *delemar* germlings and unbound proteins were removed with repeated washing. Bound proteins were separated
748 on SDS-PAGE, and identified by Western blotting using anti-biotin monoclonal antibody (Ab, top panel) and
749 the identity of the proteins were confirmed to be GRP78 (78 kDa) for nasal (A) or integrin $\beta 1$ (130 kDa) (B) by
750 using anti-GRP78 or anti-Integrin $\alpha 3\beta 1$ antibodies, respectively (bottom panels). Affinity purification of GRP78
751 (C) or integrin $\beta 1$ (D), respectively, by other Mucorales. Anti-GRP78 and anti-integrin antibodies block *R.*
752 *delemar*-mediated invasion and subsequent damage of nasal (E) and alveolar (F) epithelial cells when compared
753 to isotype matched-IgG, respectively. Both antibodies had no effect on adherence of the fungus to host cells.
754 Data in (E) and (F) are expressed as median \pm interquartile range from 3 independent experiments. Different
755 color codes are used to simplify the graph; purple, isotype IgG; green, anti-GRP78 Ab; and yellow, anti-integrin
756 $\beta 1$ Ab.

757

758 **Fig. 3. Integrin $\alpha 3\beta 1$ is required for *R. delemar*-mediated host cell invasion and damage.** *R. delemar* has
759 reduced invasion and damage of GD25 fibroblast cell line lacking integrin $\beta 1$, compared to $\beta 1$ GD25, an integrin
760 $\beta 1$ restored fibroblast cell line (A). Adhesion and invasion of GD25 and $\beta 1$ AGD25 fibroblast cell lines were
761 conducted using differential fluorescent assay, while host cell damage was carried out using ^{51}Cr release
762 method. Confocal microscopy images showing the accumulation of integrin $\alpha 3\beta 1$ around *R. delemar* during

763 infection of alveolar epithelial cells (B). Images were taken after 2.5 hours of incubation of the fungus with the
764 host cells. Anti-integrin $\alpha 3\beta 1$ monoclonal antibody block *R. delemar*-mediated invasion of alveolar epithelial
765 cells (C). Alveolar epithelial cells were incubated with 5 $\mu\text{g}/\text{ml}$ of different anti-integrins antibodies or isotype-
766 matched IgG for 1 hour prior to infecting with *R. delemar*. Data are expressed as median \pm interquartile range
767 from 3 independent experiments for (A) and (C).

768
769 **Fig. 4. Anti-integrin antibodies block activation of alveolar epithelial cell EGFR.** Representative
770 immunoblots (A) and densitometric analysis (B) show that *R. delemar* infection induced phosphorylation of
771 EGFR on tyrosine residue 1068 compared to control and anti-integrin $\beta 1$ antibody blocked it. Data in (B) are
772 mean \pm SD of three independent experiments.

773
774 **Fig. 5. CoH3 is the *R. delemar* cell-surface ligand to GRP78 on nasal epithelial cells.** Far-Western blot of
775 *R. delemar* surface proteins that bound to GRP78 (A). Affinity purification of nasal cell GRP78 by *S. cerevisiae*
776 cells expressing CoH3 identified by anti-GRP78 antibody (B). Dashed line represent cropped image from Fig.
777 2A GRP78 blot. Confocal microscopy images showing interaction of nasal epithelial GRP78 and *R. delemar*
778 CoH3 after 2.5 hours incubation shown by proximity ligation assay (PLA) (C). DAPI staining was used to
779 identify host cells. Inhibition of CoH3 expression by RNAi reduced the ability of *R. delemar* to invade (by
780 differential fluorescence) and damage (by ^{51}Cr release method) nasal epithelial cells compared with empty
781 plasmid transformed *R. delemar* (D). Anti-CoH3 antibody blocked *R. delemar*-mediated invasion of and
782 damage to nasal epithelial cells. Data in (D) and (E) are expressed as median \pm interquartile range from 3
783 independent experiments.

784
785 **Fig. 6. CoH7 is the *R. delemar* cell-surface ligand to integrin $\alpha 3\beta 1$.** Far-Western blot of *R. delemar* surface
786 proteins that bound to integrin (A). Inhibition of CoH3 expression by RNAi reduced the ability of *R. delemar*
787 to invade (by differential fluorescence) and damage (by ^{51}Cr release) alveolar epithelial cells compared with

788 empty plasmid transformed *R. delemar* (B). Data in (B) are expressed as median \pm interquartile range from 3
789 independent experiments.

790

791 **Fig. 7. DKA host factors increase nasal epithelial cell GRP78 expression and host cell susceptibility to *R.***
792 ***delemar*–mediated invasion and damage.** Nasal epithelial cells were incubated with physiologically elevated
793 concentrations of glucose, iron or BHB for 5 hours and GRP78 gene expression determined by qRT-PCR (A).
794 Elevated concentrations of glucose, iron or BHB significantly enhanced *R. delemar*-mediated nasal epithelial
795 cell invasion (B) and damage (C). Fold changes were calculated by comparison to the lowest concentration of
796 the exogenous factors used. Data are expressed as median \pm interquartile range from 3 independent
797 experiments.

798

799 **Fig. 8. DKA host factors have no effect on integrin β 1 expression levels nor they affected *R. delemar***
800 **interactions with alveolar epithelial cells.** Alveolar epithelial cells were incubated with physiologically
801 elevated concentrations of glucose, iron or BHB for 5 hours and integrin β 1 gene expression determined by
802 qRT-PCR (A). Elevated concentrations of glucose, iron or BHB had no effect on *R. delemar*–mediated alveolar
803 epithelial cell invasion (B) or subsequent damage (C). Data are expressed as median \pm interquartile range from
804 3 independent experiments.

805

806 **Fig. 9. Anti-integrin β 1 antibodies protect immunosuppressed mice from invasive pulmonary**
807 **mucormycosis due to *R. delemar*.** ICR mice (n= 10 [5 female and 5 male]/group with no difference in survival
808 among the two genders]) were immunosuppressed on day -2, +3 and +8 with cyclophosphamide and cortisone
809 acetate and infected on day 0 intratracheally with *R. delemar* (actual inhaled inoculum of 2.8×10^3 /mouse).
810 Twenty four hours post infection, mice were treated with a single dose of either a 100 μ g of an isotype-matched
811 IgG (Control) or an anti-integrin β 1 antibody. $P = 0.0006$ by Log-rank test.

812

813 **Fig. 10. A diagram showing the molecular pathogenesis of the two main manifestation of mucormycosis.**

814 *R. delemar* inhaled spores are trapped in the sinus cavity of patients with DKA due to the overexpression of
815 GRP78 on nasal epithelial cells and the interaction with fungal CotH3 resulting in rhinoorbital/cerebral
816 mucormycosis (A). In immunosuppressed patients, inhaled spores reach the alveoli and bind to integrin $\alpha3\beta1$
817 via fungal CotH7, thereby triggering activation of EGFR and subsequent invasion and pulmonary infection (B).

818

819 **Supplemental Material**

820 **Fig. S1. *R. delemar* damage of primary human alveolar epithelial cells (PAEpiC).** Damage assay time
821 points were carried out using ^{51}Cr release method. Data are expressed as median \pm interquartile range.

822

823 **Fig. S2. Expression of GRP78 and integrin during *R. delemar* infection of alveolar epithelial cells after 3
824 hours of interaction.** The expression was quantified by qRT-PCR. Data are expressed as median \pm interquartile
825 range from three independent experiments.

826

827 **Fig. S3. Co-localization of integrin $\beta 1$ and $\alpha 5$ around *R. delemar*:** Confocal microscopy images showing
828 differentially fluorescent integrin $\beta 1$ but not $\alpha 5$ around *R. delemar* germlings during infection of alveolar
829 epithelial cells. Images were taken after 2.5 hours of incubation of the fungus with the host cells.

830

831 **Fig. S4. RNAi targeting CotH7 inhibits the expression of CotH7.** *R. delemar* was transformed with an RNAi
832 construct targeting CotH7 expression or empty plasmid. Cells transformed with RNAi construct targeting
833 CotH7 demonstrated 50% reduction in CotH7 expression relative to empty plasmid-transformed *R. delemar*, as
834 determined by RT-PCR after 16 hours of incubation.

835

836 **Fig. S5. Inhibition of CotH3 had no effect on invasion of or damage to alveolar epithelial cells by *R.*
837 *delemar*.** Inhibition of CotH3 expression by RNAi did not alter the ability of *R. delemar* to adhere to, invade or
838 damage alveolar epithelial cells vs. *R. delemar* transformed with empty plasmid (A). Anti-CotH3 antibody
839 block *R. delemar* mediated adhesion and invasion but not alter damage of alveolar cells when compared to host
840 cells incubated with isotype-matched IgG (B). Adhesion and invasion assay was carried out by differential
841 fluorescence, while damage was carried out using ^{51}Cr release method. Data are expressed as median \pm
842 interquartile range from 3 independent experiments.

843

844 **Fig. S6. Inhibition of Coth7 by RNAi had no effect on *R. delemar* interactions with nasal epithelial cells.**

845 Adhesion and invasion assay was conducted by differential fluorescence using nasal cells spilt on 12-mm glass
846 coverslips, while damage assay was carried out using ^{51}Cr release assay. Data are expressed as median \pm
847 interquartile range from 3 independent experiment.

848

849 **Fig. S7. The Coth protein family.** Phylogenetic tree and relative distance of *R. delemar* Coth proteins (A),
850 and their percent identity (B).

851

852 **Fig. S8. Alignment results between Coth3 peptide (that has been used for anti-Coth3 production) and**
853 **Coth7.** Multiple Sequence Comparison by Log- Expectation (MUSCLE) online tool used to perfume sequence
854 alignment between 16-mer Coth3 and Coth7 protein using cluster 12.1 algorithm.

855

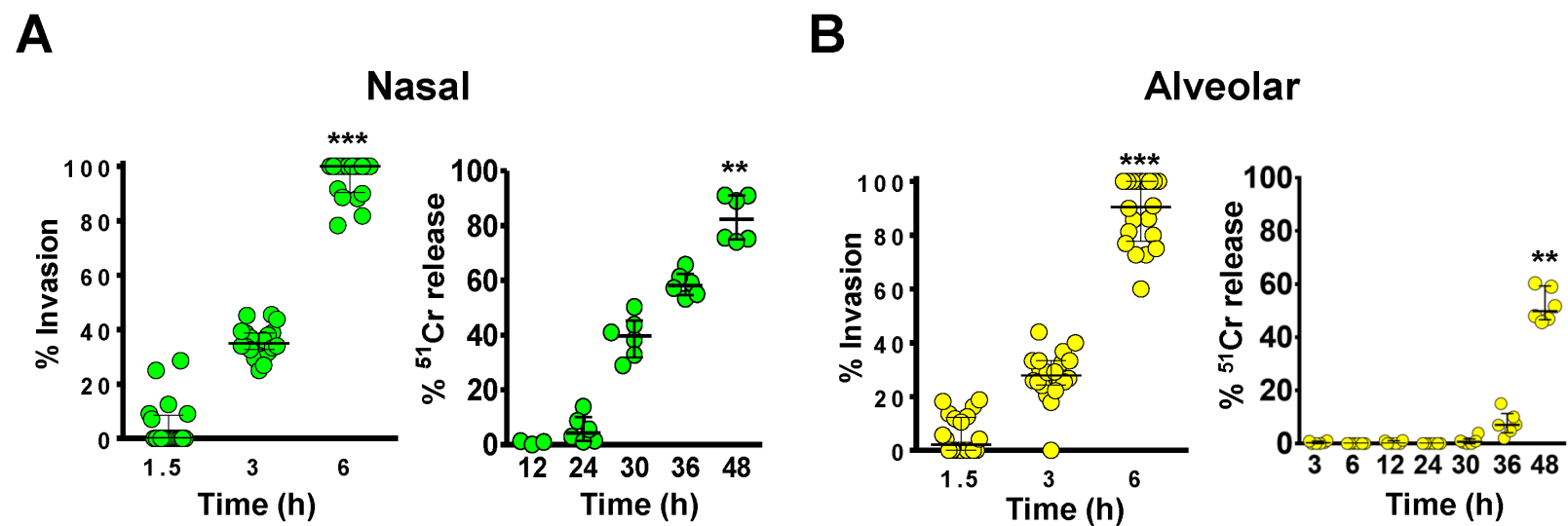


Fig. 1. *R. delemar*-mediated invasion and damage of nasal and alveolar epithelial cells. *R. delemar* invasion of nasal (A) or alveolar (B) epithelial cells was determined using differential fluorescent assay by staining with 1% Uvitex for 1 hour, while damage assay was performed using ⁵¹Cr release method. *** $P < 0.0001$ and ** $P < 0.001$ compared to the first time point in each panel. Data presented as median \pm interquartile range from 3 independent experiments.

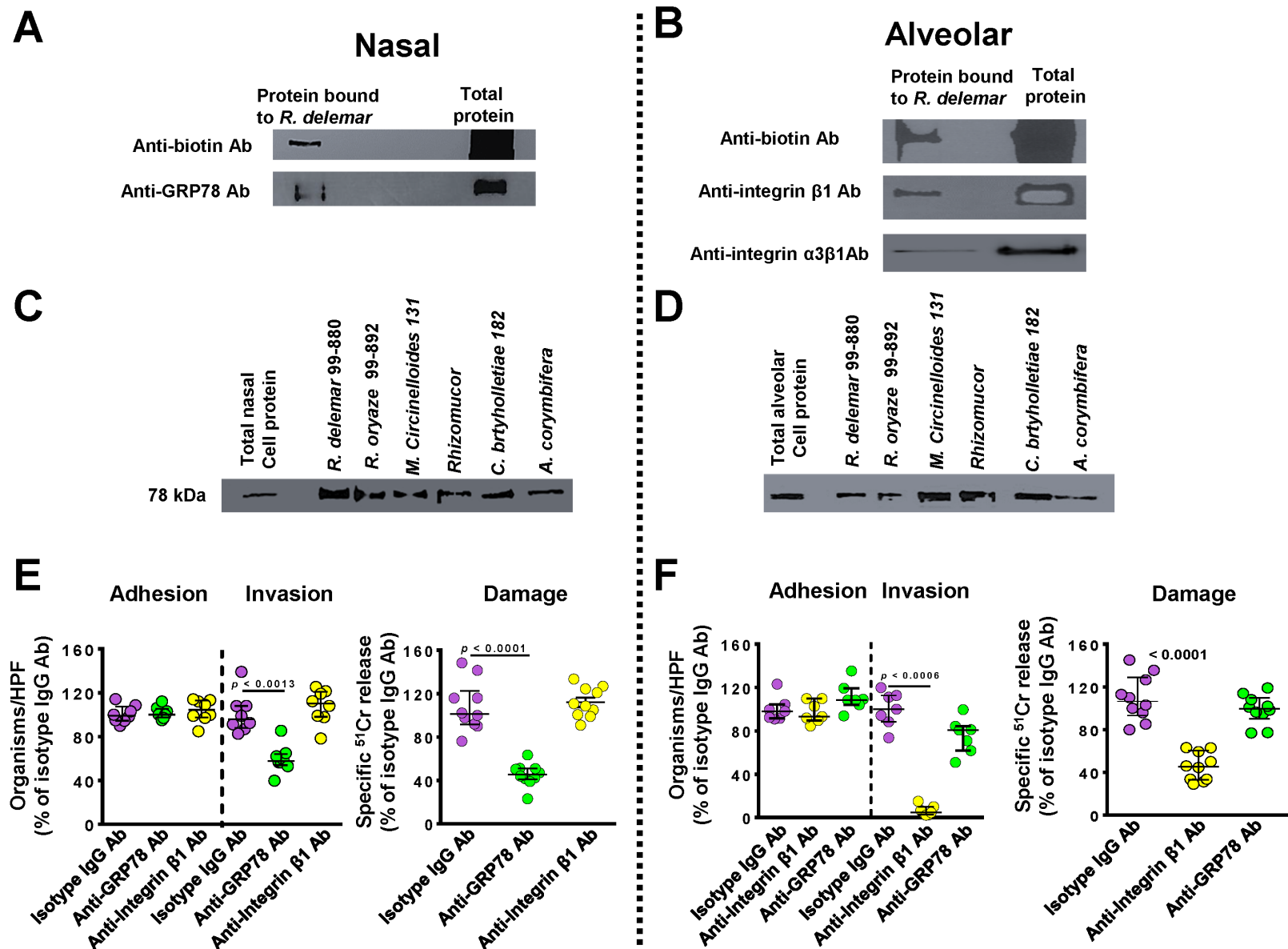


Fig. 2. GRP78 is a nasal epithelial cell receptor, while integrin α 3 β 1 is an alveolar epithelial cell receptor during *Mucorales* interaction. Biotinylated nasal (A) or alveolar (B) epithelial cells were incubated with *R. delemar* germlings and unbound proteins were removed with repeated washing. Bound proteins were separated on SDS-PAGE, and identified by Western blotting using anti-biotin monoclonal antibody (Ab, top panel) and the identity of the proteins were confirmed to be GRP78 (78 kDa) for nasal (A) or integrin β 1 (130 kDa) (B) by using anti-GRP78 or anti-Integrin α 3 β 1 antibodies, respectively (bottom panels). Affinity purification of GRP78 (C) or integrin β 1 (D), respectively, by other *Mucorales*. Anti-GRP78 and anti-integrin antibodies block *R. delemar*-mediated invasion and subsequent damage of nasal (E) and alveolar (F) epithelial cells when compared to isotype matched-IgG, respectively. Both antibodies had no effect on adherence of the fungus to host cells. Data in (E) and (F) are expressed as median \pm interquartile range from 3 independent experiments. Different color codes are used to simplify the graph; purple, isotype IgG; green, anti-GRP78 Ab; and yellow, anti-integrin β 1 Ab.

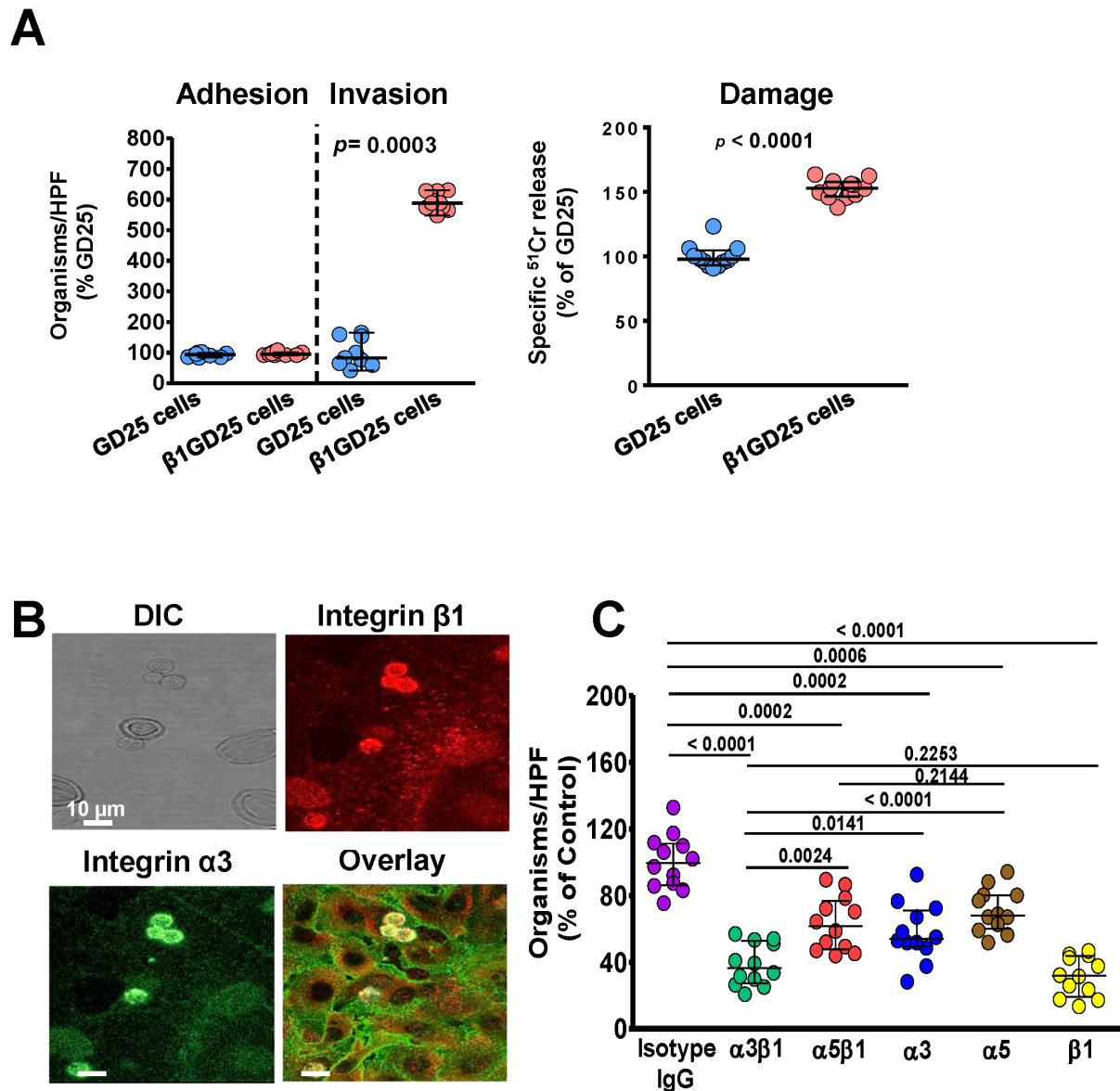
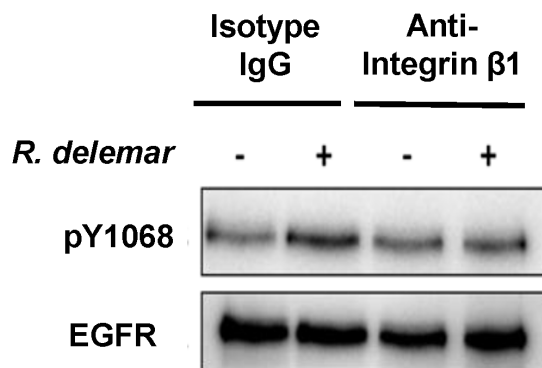


Fig. 3. Integrin $\alpha3\beta1$ is required for *R. delemar*-mediated host cell invasion and damage. *R. delemar* has reduced invasion and damage of GD25 fibroblast cell line lacking integrin $\beta1$, compared to $\beta1$ GD25, an integrin $\beta1$ restored fibroblast cell line (A). Adhesion and invasion of GD25 and $\beta1$ GD25 fibroblast cell lines were conducted using differential fluorescent assay, while host cell damage was carried out using ^{51}Cr release method. Confocal microscopy images showing the accumulation of integrin $\alpha3\beta1$ around *R. delemar* during infection of alveolar epithelial cells (B). Images were taken after 2.5 hours of incubation of the fungus with the host cells. Anti-integrin $\alpha3\beta1$ monoclonal antibody block *R. delemar*-mediated invasion of alveolar epithelial cells (C). Alveolar epithelial cells were incubated with 5 $\mu\text{g}/\text{ml}$ of different anti-integrins antibodies or isotype-matched IgG for 1 hour prior to infecting with *R. delemar*. Data are expressed as median \pm interquartile range from 3 independent experiments for (A) and (C).

A



B

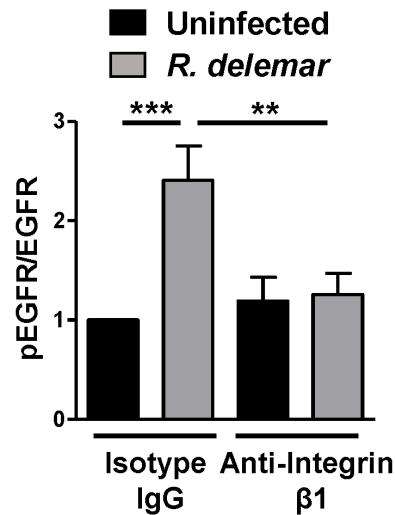


Fig. 4. Anti-integrin antibodies block activation of alveolar epithelial cell EGFR. Representative immunoblots (A) and densitometric analysis (B) show that *R. delemar* infection induced phosphorylation of EGFR on tyrosine residue 1068 compared to control and anti-integrin β1 antibody blocked it. Data in (B) are mean \pm SD of three independent experiments.

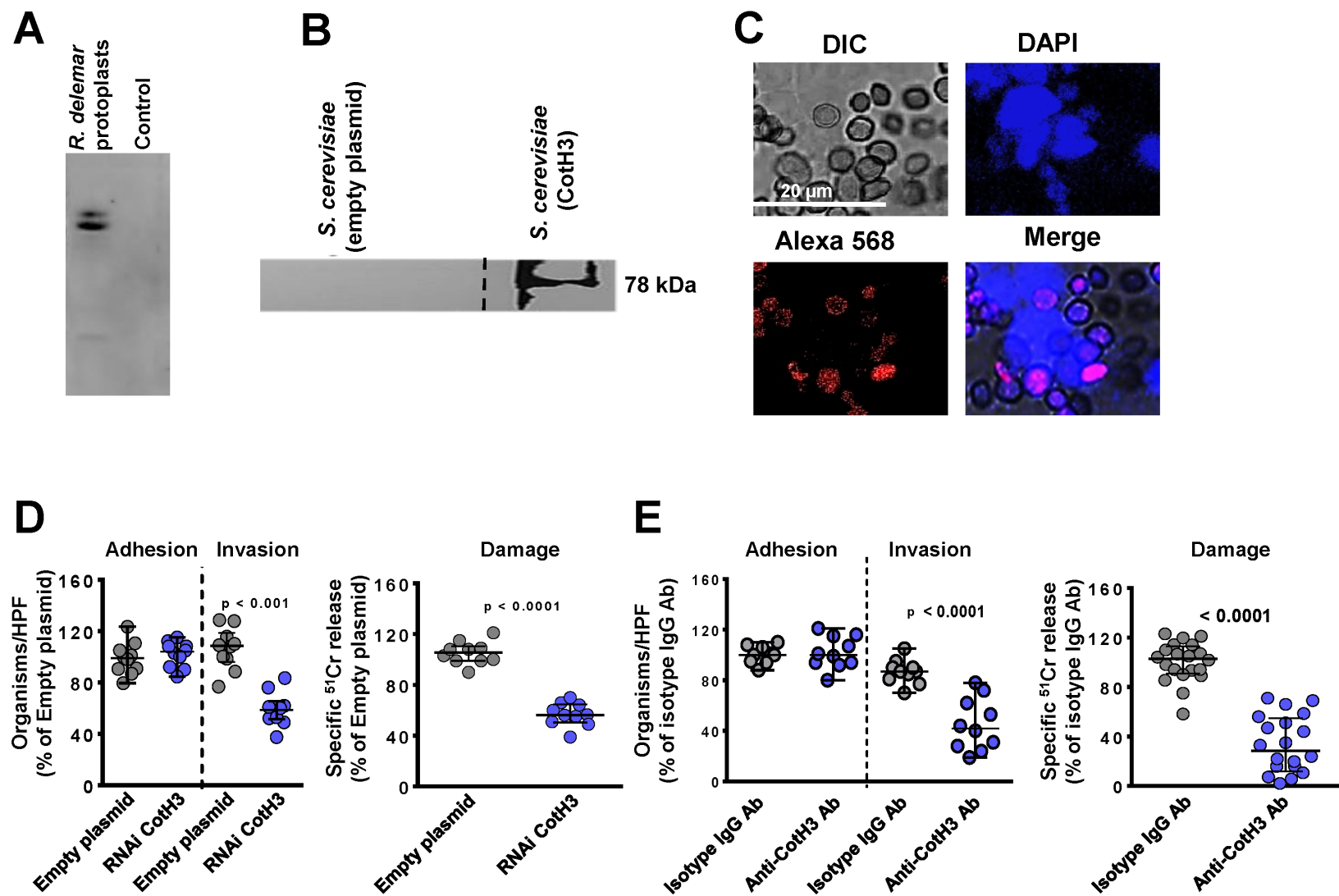


Fig. 5. Coth3 is the *R. delemar* cell-surface ligand to GRP78 on nasal epithelial cells. Far-Western blot of *R. delemar* surface proteins that bound to GRP78 (A). Affinity purification of nasal cell GRP78 by *S. cerevisiae* cells expressing Coth3 identified by anti-GRP78 antibody (B). Dashed line represent cropped image from Fig. 2A GRP78 blot. Confocal microscopy images showing interaction of nasal epithelial GRP78 and *R. delemar* Coth3 after 2.5 hours incubation shown by proximity ligation assay (PLA) (C). DAPI staining was used to identify host cells. Inhibition of Coth3 expression by RNAi reduced the ability of *R. delemar* to invade (by differential fluorescence) and damage (by ^{51}Cr release method) nasal epithelial cells compared with empty plasmid transformed *R. delemar* (D). Anti-Coth3 antibody blocked *R. delemar*-mediated invasion of and damage to nasal epithelial cells. Data in (D) and (E) are expressed as median \pm interquartile range from 3 independent experiments.

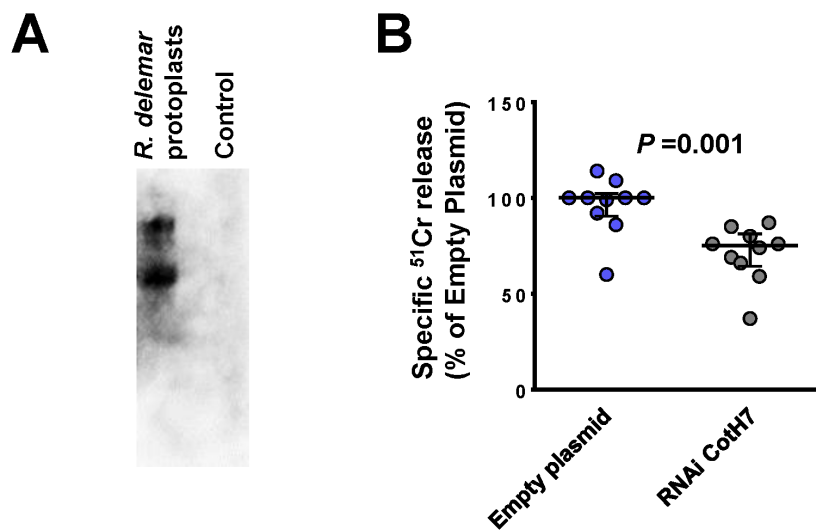


Fig. 6. CotH7 is the *R. delemar* cell-surface ligand to integrin $\alpha 3\beta 1$. Far-Western blot of *R. delemar* surface proteins that bound to integrin (A). Inhibition of CotH3 expression by RNAi reduced the ability of *R. delemar* to invade (by differential fluorescence) and damage (by ⁵¹Cr release) alveolar epithelial cells compared with empty plasmid transformed *R. delemar* (B). Data in (B) are expressed as median \pm interquartile range from 3 independent experiments.

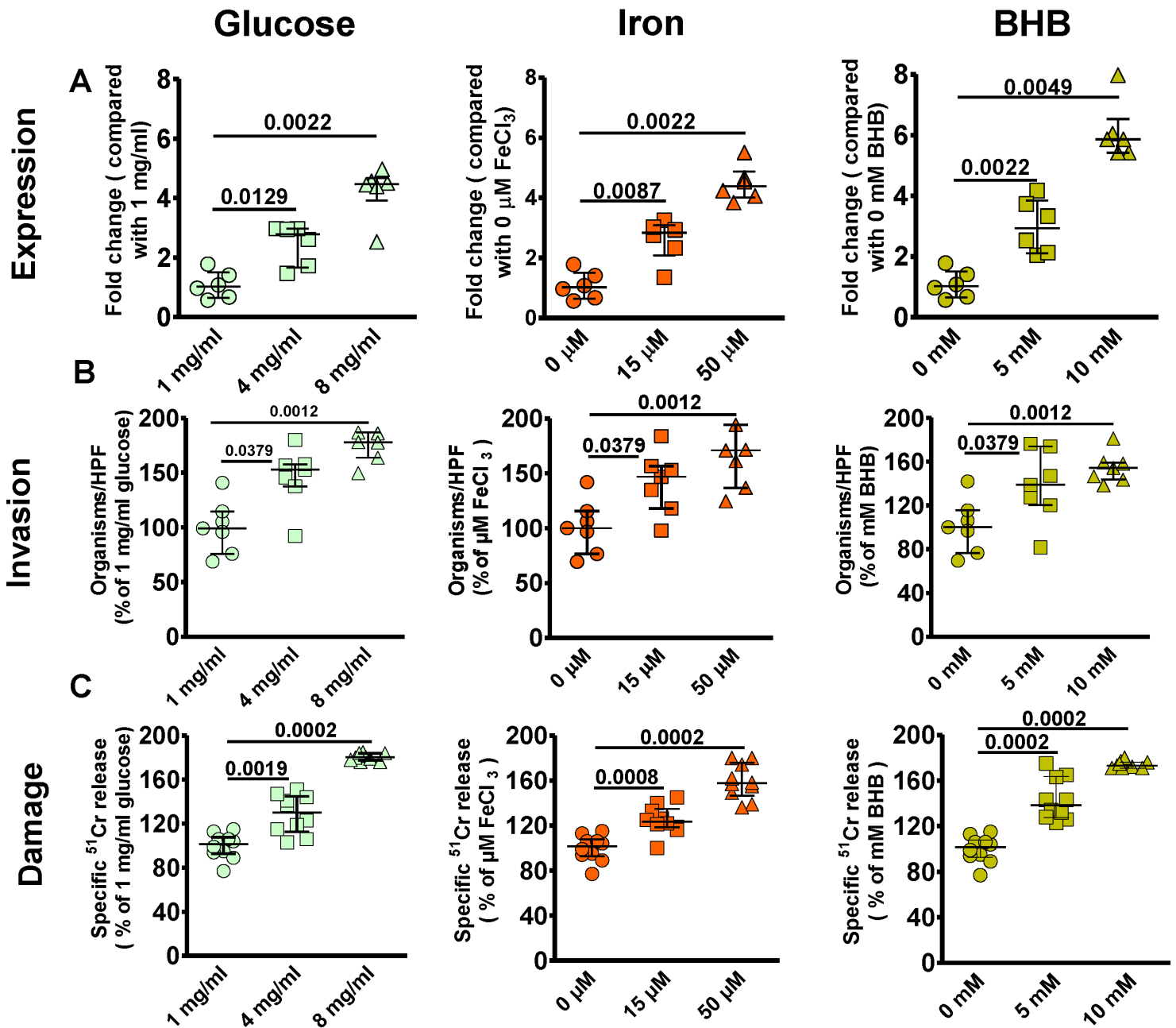


Fig. 7. DKA host factors increase nasal epithelial cell GRP78 expression and host cell susceptibility to *R. delemar*-mediated invasion and damage. Nasal epithelial cells were incubated with physiologically elevated concentrations of glucose, iron or BHB for 5 hours and GRP78 gene expression determined by qRT-PCR (A). Elevated concentrations of glucose, iron or BHB significantly enhanced *R. delemar*-mediated nasal epithelial cell invasion (B) and damage (C). Fold changes were calculated by comparison to the lowest concentration of the exogenous factors used. Data are expressed as median \pm interquartile range from 3 independent experiments.

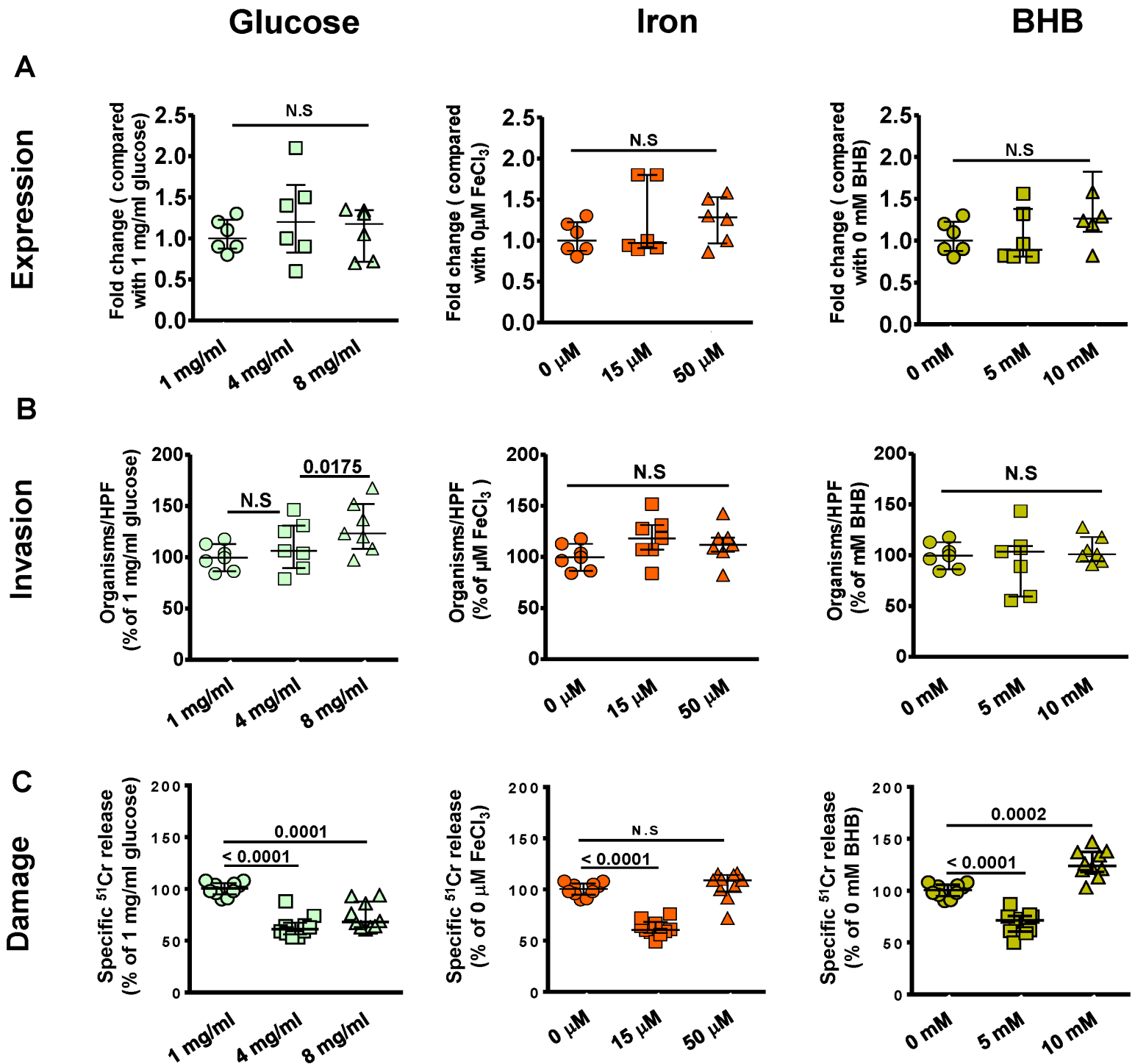


Fig. 8. DKA host factors have no effect on integrin β 1 expression levels nor they affected *R. delemar* interactions with alveolar epithelial cells. Alveolar epithelial cells were incubated with physiologically elevated concentrations of glucose, iron or BHB for 5 hours and integrin β 1 gene expression determined by qRT-PCR (A). Elevated concentrations of glucose, iron or BHB had no effect on *R. delemar*-mediated alveolar epithelial cell invasion (B) or subsequent damage (C). Data are expressed as median \pm interquartile range from 3 independent experiments.

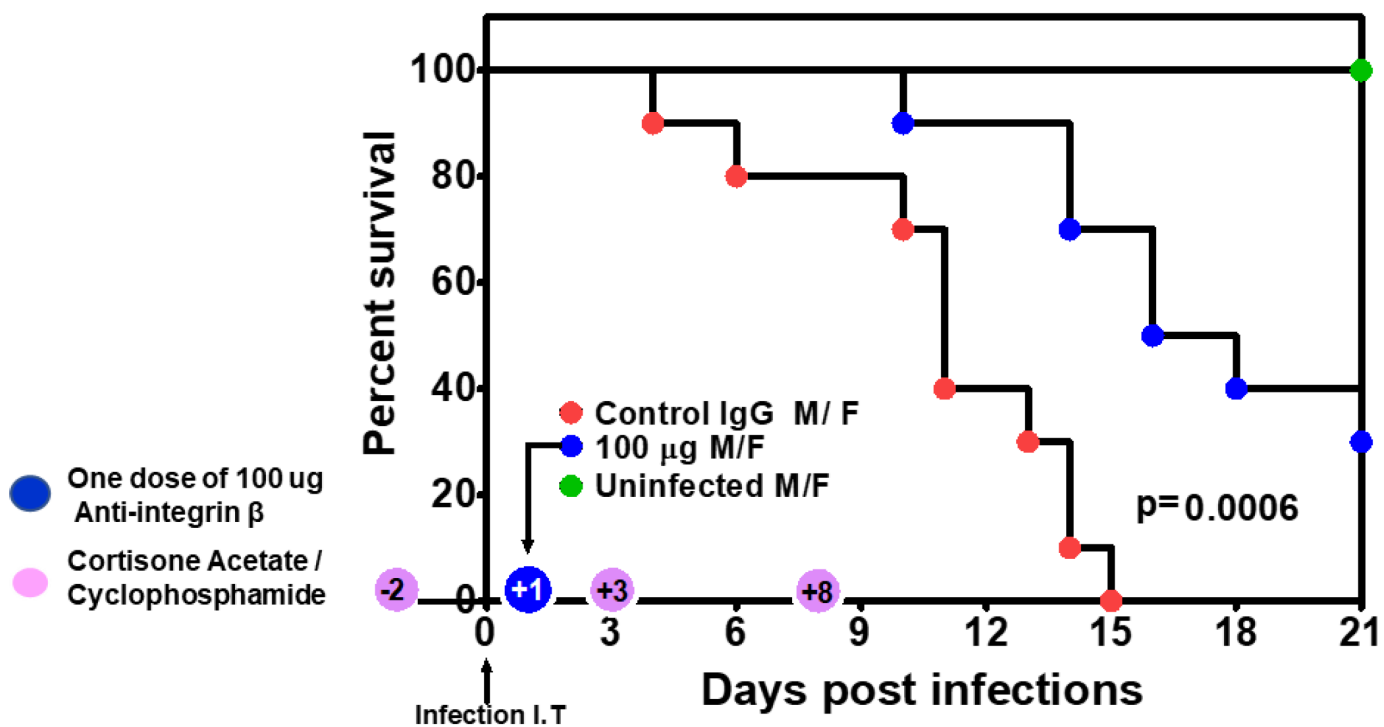


Fig. 9. Anti-integrin β 1 antibodies protect immunosuppressed mice from invasive pulmonary mucormycosis due to *R. delemar*. ICR mice (n= 10 [5 female and 5 male]/group with no difference in survival among the two genders) were immunosuppressed on day -2, +3 and +8 with cyclophosphamide and cortisone acetate and infected on day 0 intratracheally with *R. delemar* (actual inhaled inoculum of 2.8×10^3 /mouse). Twenty four hours post infection, mice were treated with a single dose of either a 100 μ g of an isotype-matched IgG (Control) or an anti-integrin β 1 antibody. $P = 0.0006$ by Log-rank test.

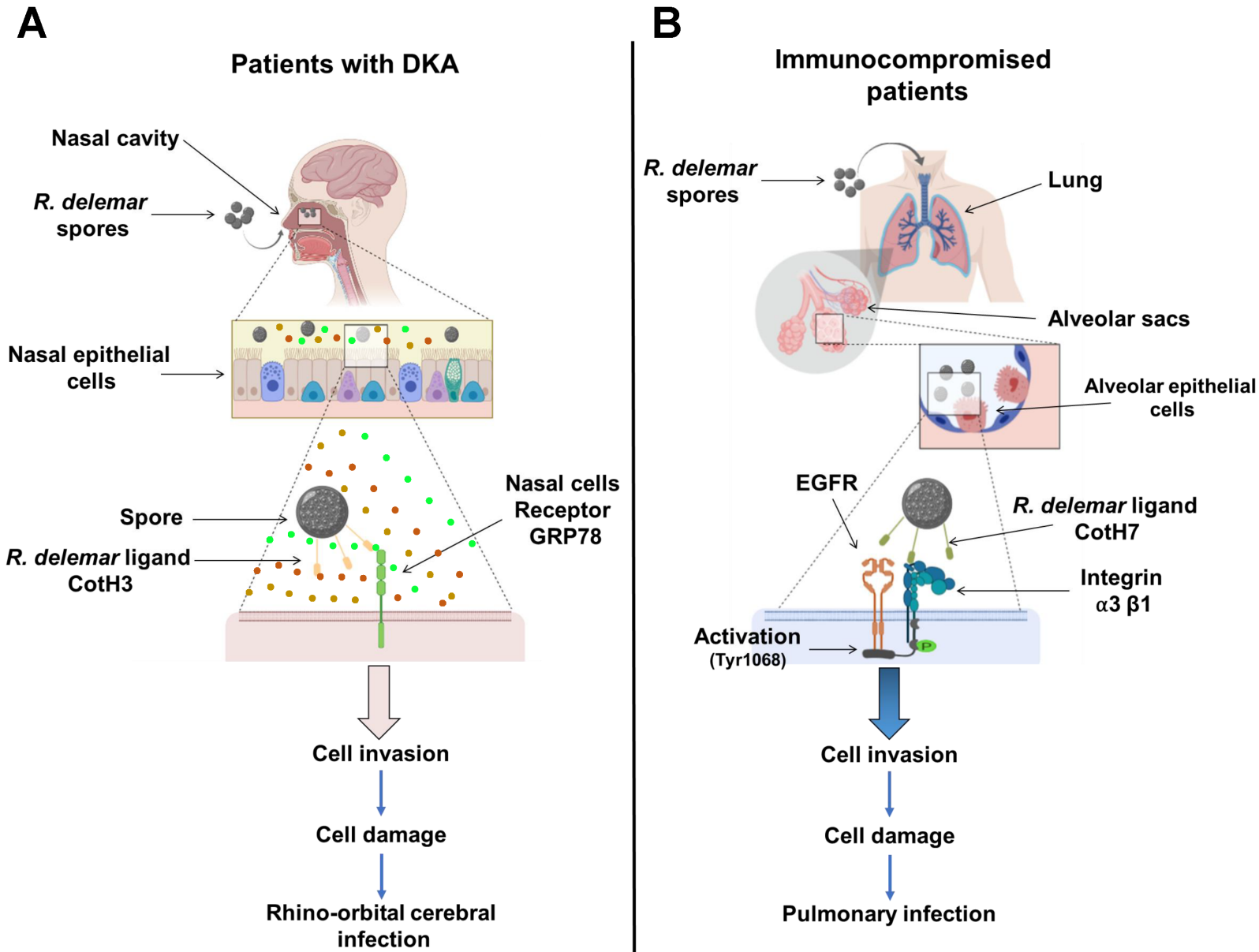


Fig. 10. A diagram showing the molecular pathogenesis of the two main manifestation of mucormycosis. *R. delemar* inhaled spores are trapped in the sinus cavity of patients with DKA due to the overexpression of GRP78 on nasal epithelial cells and the interaction with fungal Coth3 resulting in rhinoorbital/cerebral mucormycosis (A). In immunosuppressed patients, inhaled spores reach the alveoli and bind to integrin $\alpha 3 \beta 1$ via fungal Coth7, thereby triggering activation of EGFR and subsequent invasion and pulmonary infection (B).